AWARD NUMBER: W81XWH-13-1-0193

TITLE: Clinical Development of Gamitrinib, a Novel Mitochondrial-Targeted Small Molecule Hsp90 Inhibitor

PRINCIPAL INVESTIGATOR: Dario C. Altieri

CONTRACTING ORGANIZATION: Wistar Institute of Anatomy & Biology
Philadelphia, PA 19104

REPORT DATE: September 2014

TYPE OF REPORT: Annual Report

PREPARED FOR: U.S. Army Medical Research and Materiel Command
Fort Detrick, Maryland 21702-5012

REPORT DOCUMENTATION PAGE

Form Approved
OMB No. 0704-0188

1. REPORT DATE *(DD-MM-YYYY)*	2. REPORT TYPE	3. DATES COVERED *(From - To)*
September 2014	Annual Report	01Sep2013-31Aug2014

4. TITLE AND SUBTITLE
Clinical Development of Gamitrinib, a Novel Mitochondrial-Targeted Small Molecule Hsp90 Inhibitor

5a. CONTRACT NUMBER

5b. GRANT NUMBER
W81XWH-13-1-0193

5c. PROGRAM ELEMENT NUMBER

6. AUTHOR(S)
Dario C. Altieri

email: daltieri@wistar.org

5d. PROJECT NUMBER

5e. TASK NUMBER

5f. WORK UNIT NUMBER

7. PERFORMING ORGANIZATION NAME(S) AND ADDRESS(ES)
Wistar Institute of Anatomy & Biology

Philadelphia, PA 19104

8. PERFORMING ORGANIZATION REPORT NUMBER

9. SPONSORING / MONITORING AGENCY NAME(S) AND ADDRESS(ES)
U.S. Army Medical Research and Materiel Command
Fort Detrick, Maryland 21702-5012

10. SPONSOR/MONITOR'S ACRONYM(S)

11. SPONSOR/MONITOR'S REPORT NUMBER(S)

12. DISTRIBUTION / AVAILABILITY STATEMENT
Approved for Public Release; Unlimited Distribution

13. SUPPLEMENTARY NOTES

14. ABSTRACT
Considerable progress has been made during the past budget cycle on all of the specific tasks set forth in the SOW for the present proposal. The overarching goal of Specific Aim 1 (months 0-12 of award) has been accomplished, with the identification of a novel metabolomics protein signature of Gamitrinib anticancer activity, in vivo (i), the characterization of protein biomarkers of Gamitrinib function in genetic models of prostate cancer (ii), and the further biochemical characterization of the target of Gamitrinib, TRAP-,1 in tumor bioenergetics and metabolic reprogramming (iii). Altogether, the work supported by the present award led to the publication of two articles directly relevant to the scopes of the present SOW (Chae et al Nat Comm. 4:2139; Lisanti et al Cell Rep 617:7), the submission for publication of a third original article (Ghosh et al –submitted), and the presentation of some of the SOW research findings at a national conference (Keystone Conference on Mitochondrial Dynamics and Physiology, Santa Fe, NM -18/2/2014 – 23/2/2014).

15. SUBJECT TERMS
Mitochondria, oxidative phosphorylation, Hsp90, advanced prostate cancer, Gamitrinib

16. SECURITY CLASSIFICATION OF:			17. LIMITATION OF ABSTRACT	18. NUMBER OF PAGES	19a. NAME OF RESPONSIBLE PERSON
a. REPORT	b. ABSTRACT	c. THIS PAGE			USAMRMC
U	U	U	UU	24	19b. TELEPHONE NUMBER *(include area code)*

TABLE OF CONTENTS

1. **INTRODUCTION**. The present research project is designed to reach a complete preclinical characterization (formulation studies, pharmacokinetics analysis, toxicology profile and identification and validation of suitable biomarkers) of Gamitrinib (GA mitochondrial matrix inhibitor), a first-in-class, mitochondrial-targeted small molecule inhibitor of Heat Shock Protein-90 (Hsp90) chaperones. Extensive preliminary data in support of the application have demonstrated that Gamitrinib has a unique mechanism of action, penetrating the mitochondria and selectively inhibiting the ATPase activity of a pool of Hsp90 and Hsp90-homolog TRAP-1 (TNFR-Associated Protein-1, TRAP-1) chaperones localized within the mitochondrial matrix and inner membrane. In turn, this causes catastrophic loss of protein folding quality control selectively within mitochondria, collapse of tumor bioenergetics, massive activation of apoptosis and potent single-agent and combination cytotoxic anticancer activity, in vivo. As Hsp90 chaperones are selectively enriched in tumor mitochondria, as opposed to normal tissues, Gamitrinib has shown good tolerability in preclinical xenograft and genetic tumor models, in vivo. The overarching goal of the proposal is to complete all of the preclinical characterization of Gamitrinib in order to support filing of an Investigational New Drug (IND) Application with the US Food and Drug Administration (FDA). This will fulfill key regulatory requirements in anticipation of the clinical testing of Gamitrinib in patients with advanced, castrate-resistant and metastatic prostate cancer.

2. **KEYWORDS**. Mitochondria, oxidative phosphorylation, Hsp90, metabolomics, advanced prostate cancer, Gamitrinib

3. **ACCOMPLISHMENTS**.

- *What were the major goals and objectives of the project?* Consistent with the mechanism of anticancer activity of Gamitrinib, which involves disabling of mitochondrial bioenergetics (i) and activation of mitochondrial apoptosis (ii), the major goal of this project for months 0-12 of the award was: **To develop a proteomics and metabolomics biomarker of Gamitrinib mitochondriotoxic therapy, in vivo**. This included the specific objectives of: **Identification of proteomics and metabolomics signatures as a biomarker of Gamitrinib anticancer activity** (i), and **Evaluation of proteomics and metabolomics signatures as biomarkers of Gamitrinib anticancer activity, in vivo** (ii).

- *What was accomplished under these goals?*

1. Major activities.

a) Establishment and validation of a novel biochemical method to identify mitochondrial proteins that require Hsp90 chaperone activity for stability and/or proper folding.

b) Validation of independent and complementary approaches of 1D proteomics (i) and Stable Isotope Labeling of Amino Acids in Culture (SILAC) (ii) to identify a "mitochondrial Hsp90 proteome", comprising organelle-localized molecules that require chaperone activity for proper folding, stability and biochemical function.

c) Characterization of a global metabolic gene signature as a surrogate biomarker of Gamitrinib anticancer activity in prostate cancer PC3 cells derived from quantification of 301 individual biochemicals intercalated in multiple bioenergetics pathways.

d) Identification of Succinate Dehydrogenase B (SDHB) as a key metabolic target of Gamitrinib anticancer activity in mitochondrial oxidative phosphorylation.

e) Validation of a biomarker signature of Gamitrinib anticancer activity in a genetic model of prostate cancer (TRAMP –Transgenic Adenocarcinoma of the Mouse Prostate mice).

f) Generation and characterization of TRAP-1 knockout mice as a first model of chaperone-regulated dynamic mitochondrial metabolic reprogramming.

2. Specific objectives.

Subtask 1 - *Proteomics identification of mitochondrial proteins that require Hsp90 for proper folding* (*Mitochondrial Hsp90 Proteome*). To carry out these studies, we first optimized a new biochemical method to detect proteins that require mitochondrial Hsp90 chaperone activity for proper folding and/or stability. For these experiments, we exposed androgen-independent prostate cancer PC3 cells to non-toxic concentrations of Gamitrinib (1-5 μM) or vehicle (DMSO), isolated mitochondrial proteins, and treated the samples with increasing detergent concentrations (CHAPS or NP-40) followed by quantification of soluble/insoluble material by SDS-PAGE and Western blotting. After validation of the method, unknown proteins remaining in the insoluble fractions in response to Gamitrinib treatment (i.e., aggregated and misfolded proteins) were identified by 1D proteomics.

As an independent approach to comprehensively map a "mitochondrial Hsp90 proteome", we also optimized a new proteomics approach using Stable Isotope Labeling of Amino Acids in Culture (SILAC). For these experiments, we labeled control or Gamitrinib-treated prostate cancer PC3 cells with heavy and light atoms, mixed the two differentially labeled cultures together and identified differentially represented proteins by unbiased proteomics. Using a highly stringent cutoff of 3-fold differences in protein folding/aggregation between control and Gamitrinib treatment, these two complementary proteomics approaches allowed the identification of 44 proteins in mitochondria that required Hsp90 and TRAP-1 chaperone activity for proper folding, stability and function.

Subtask 2 - *Metabolomics screening of mitochondrial Hsp90-directed bioenergetics*. Consistent with the SOW, we carried out additional experiments to identify a global metabolomics signature as a biomarker of Gamitrinib inhibition of tumor bioenergetics. For these studies, we incubated androgen-independent prostate cancer PC3 cells with non-cytotoxic concentrations of Gamitrinib (1-5 μM) or vehicle (DMSO), and treated cells were analyzed in a global metabolomics screen that quantifies changes in expression levels of 301 metabolites intercalated in various cellular bioenergetics pathways.

Major task 2. *Evaluation of proteomics and metabolomics signatures as biomarkers of Gamitrinib anticancer activity, in vivo*. To validate the suitability of changes in tumor bioenergetics as a biomarker of Gamitrinib anticancer activity, in vivo, we carried out studies in a genetic model of prostate cancer using immunocompetent TRAMP (Transgenic Adenocarcinoma of the Mouse Prostate) mice. For these experiments, TRAMP mice were divided into two age groups to received Gamitrinib monotherapy at 5 mg/kg in cremophor as i.p. injections, with the schedule 3 days on/2 days off. Mice in group 1 (short-term treatment) received Gamitrinib starting at 21.9 weeks of age for 3 weeks (24.9 weeks of age), with analysis of primary and metastatic prostate cancer as end point. Animals in group 2 (long-term treatment) were started on Gamitrinib at 14.7 weeks of age for 5 weeks (19.7 weeks of age), and assessed histologically for primary prostate cancer growth, development of prostatic intraepithelial neoplasia (PIN), localized inflammation and expression of a combined biomarker signature of metabolic starvation, cellular stress response and autophagy. These experiments were partially supported by the present award.

To further characterize the role of mitochondrial Hsp90 chaperones as targets of Gamitrinib anticancer activity, we generated TRAP-1 knockout mice. Using gene-trap technology, we obtained mouse ES cells in which a β-galactosidase gene disrupts the TRAP-1 locus on chromosome 16, downstream of exon 1. Transfer of TRAP-1-targeted zygotes into C57Bl/6 pseudopregnant recipient mice generated TRAP-1 knockout animals. In genotyping experiments, PCR products of 565 nt, or, conversely, 1,148 nt identified the wild-type (WT) TRAP-1 allele or the β-galactosidase (LacZ)-containing allele, respectively. TRAP-1 knockout (TRAP-1$^{-/-}$) mice were born viable, fertile, and at expected Mendelian rates for both genders. Analysis of tissues from TRAP-1$^{-/-}$ mice, including liver, kidney, uterus, spleen, brain, heart, and testis confirmed the absence of TRAP-1 protein, compared to WT littermates, by Western blotting. Control and TRAP-1$^{-/-}$ mice were extensively analyzed for mitochondrial and bioenergetics functions. These experiments were partially supported by the present award. These experiments were partially supported by the present award.

3. Significant results or key outcomes.

Using the combined studies of 1D and SILAC proteomics, we identified a discrete "mitochondrial Hsp90 proteome" comprising molecules that require the chaperone activity for proper folding and activity. These proteins were intercalated in virtually every mitochondrial function, and comprised transcription factors *TFB1M* and *TFB2M* involved in mitochondrial gene expression and glucose homeostasis, ribosomal proteins associated with RNA translation (*MRPLs, MTG1, ERAL1*), regulators of purine biosynthesis and the methyl cycle (*MTHFD2*), and effectors of oxidative phosphorylation, including *SDHB*, *IDH3G, NDUFS3*, *PDHB*, *MDH2*. Mitochondrial proteins participating in redox status and detoxification pathways (*PRDX6, POLDIP2, CYB5R1, ETHE1*) were also identified in the mitochondrial Hsp90 proteome (Figure 1).

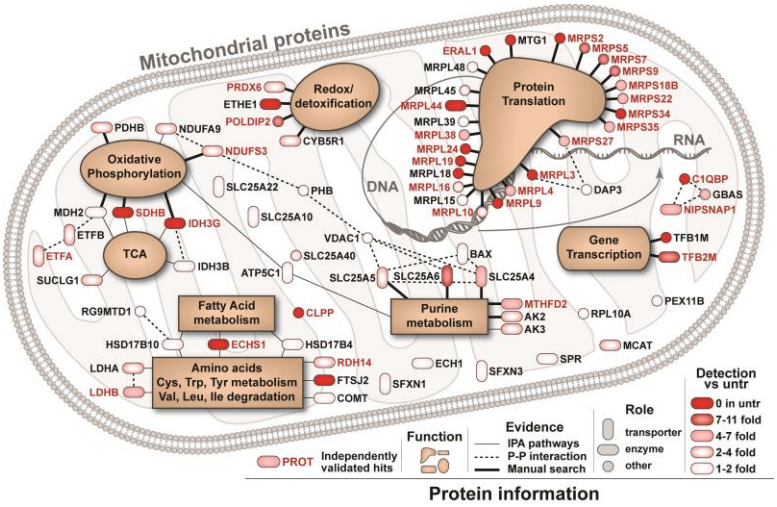

Figure 1. *Proteomics identification of the mitochondrial Hsp90 proteome as the target of Gamitrinib anticancer activity*. See text for description of specific mitochondrial proteins that require Hsp90/TRAP-1 chaperone activity for stability and/or function.

To validate experimentally the mitochondrial Hsp90 proteome, we next carried out a global metabolomics screen of Gamitrinib-treated PC3 cells. In these experiments, Gamitrinib caused global bioenergetics defects compared to vehicle-treated cultures. These included aberrant accumulation of citric acid cycle metabolites, succinate, fumarate and malate, pointing to extensive defects in oxidative phosphorylation (Figure 2), deregulated fatty acid metabolism, leading to increased long chain fatty acid transport into mitochondria, aberrations in branched chain amino acid metabolism, and changes in redox status (Figure 2). Gamitrinib-targeted cells exhibited additional defects in the metabolism of cholesterol, purine, and arginine processing (Figure 2). Consistent with induction of metabolic starvation, Gamitrinib treatment increased the AMP/ATP ratio in prostate cancer cells, induced phosphorylation of the energy sensor, AMP-activated kinase (AMPK), a key marker of cellular starvation, and inhibited mammalian target of Rapamycin (mTORC1) signaling (Figure 2).

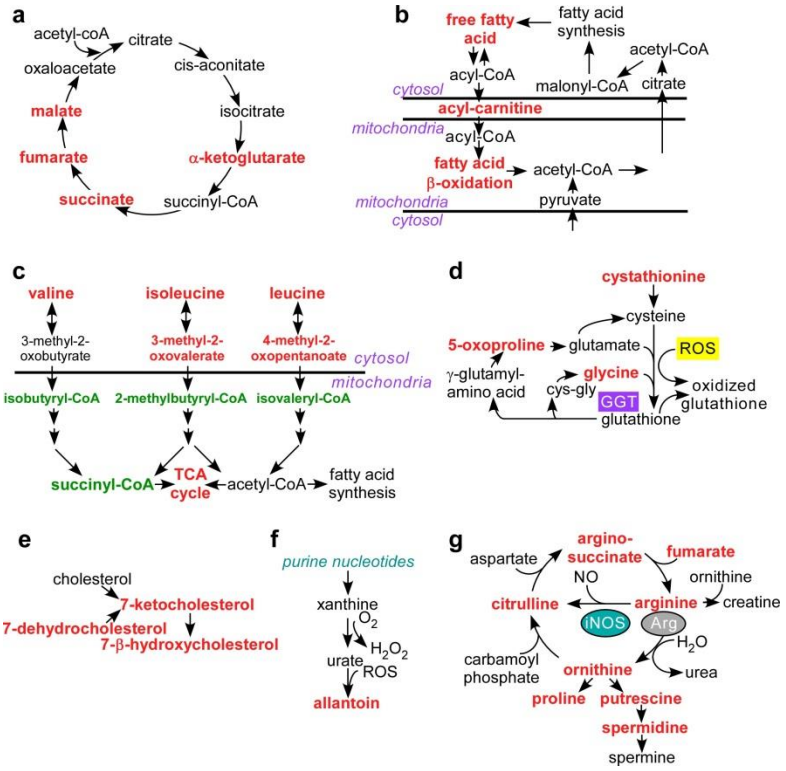

Figure 2. *Global metabolomics signature of Gamitrinib anticancer activity*. **a**, TCA cycle (oxidative phosphorylation); **b**, lipid b-oxidation; **c**, branched chain amino acid metabolism; **d**, Redox status; **e**, cholesterol metabolism; **f**, purine synthesis; **g**, arginine metabolism. *Red*, increased expression of metabolites; *green*, decreased expression of metabolites. Only statistically significant changes are shown ($p<0.05$).

These results have been published: Chae et al. (2013) *Landscape of the mitochondrial Hsp90 proteome in tumors*. **Nature Commun**. 4:2139.

Consistent with the ability of Gamitrinib to induce a phenotype of metabolic starvation with activation of AMPK and stimulation of autophagy, we next carried out in vivo studies in Gamitrinib-treated TRAMP mice. In this model, fully immunocompetent TRAMP mice express the large T antigen oncogene in the prostatic epithelium under the control of the probasin promoter and develop prostatic intraepithelial neoplasia (PIN), invasive prostate cancer and metastatic disease. Systemic treatment with Gamitrinib inhibited localized and metastatic prostate cancer in TRAMP mice. In addition, histological analysis confirmed that Gamitrinib-treated TRAMP mice exhibited a biomarker signature of cellular starvation, with increased expression of phosphorylated AMPK (Thr172) (i), induction of autophagy based on conversion of the dynamin light chain 3 (LC3-II) protein to a lipidated form (ii), and upregulation of the endoplasmic reticulum (ER) stress marker, Grp78 (iii) (Figure 3).

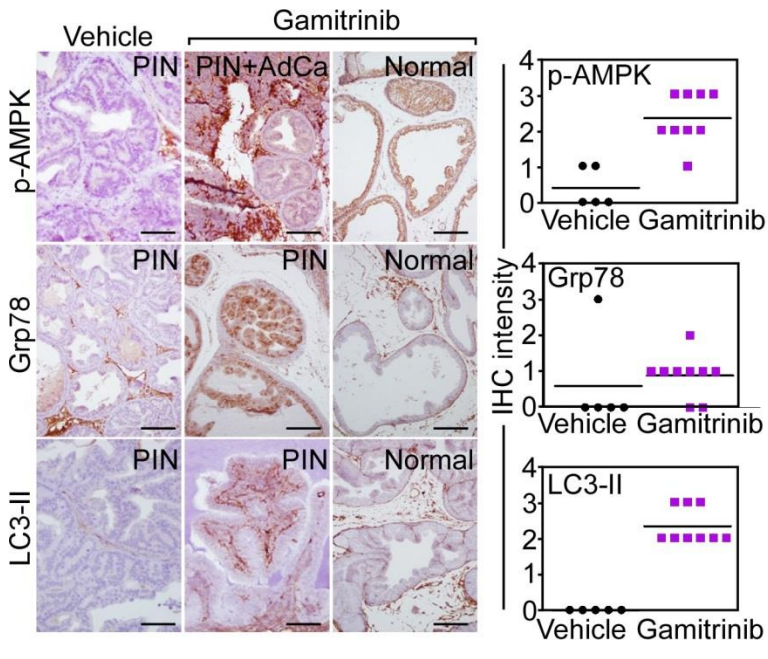

Figure 3. *Characterization of a Gamitrinib biomarker signature of anticancer activity, in vitro*. TRAMP mice were treated systemically with Gamitrinib with the 3 days/2 days off schedule, and tissues were analyzed histologically for changes in expression of phosphorylated (p) AMPK (*top*), ER stress marker, Grp78 (*middle*) or autophagy (LC3-II conversion, *bottom*). Right panels, quantification of immunohistochemistry score for the indicated markers.

To further characterize the impact of mitochondrial Hsp90s in cellular bioenergetics, in vivo, we next generated mice deficient in TRAP-1. This is a mitochondrial-localized Hsp90-like chaperone targeted by Gamitrinib, and contributing to organelle homeostasis. TRAP-1 knockout mice were born viable, fertile and at expected Mendelian rates for both genders. However, TRAP-1 deletion resulted in major compensatory responses in targeted mice characterized by transcriptional upregulation of virtually every metabolic effector of oxidative

phosphorylation and glycolysis. In turn, this resulted in aberrantly increased oxidative phosphorylation, deregulated cellular respiration, higher production of reactive oxygen species (ROS) and a general bioenergetics switch towards anaerobic glycolysis. This phenotype of metabolic reprogramming was dramatically evident when wild type (WT) and TRAP-1 knockout mice were analyzed by ^{18}F-FDG Positron Emission Tomography (PET). In these experiments, TRAP-1 knockout mice exhibited a 2- to 3-fold increase in standardized uptake values (SUVs) of the radioactive tracer in the liver, compared to WT littermates, as determined 1 h postinjection of ^{18}F-FDG (Figure 4).

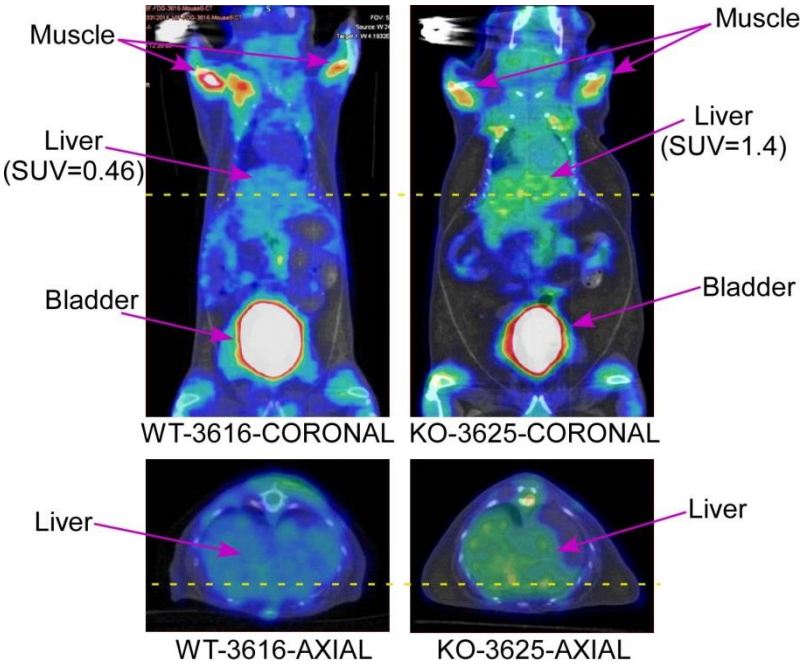

Figure 4. *^{18}F-FDG PET analysis of WT and TRAP-1 knockout (KO) mice*. The standardized uptake values (SUV) in the liver of each genotype are indicated. Coronal (*top*) and axial (*bottom*) scans are shown.

These results have been published: Lisanti et al (2014) *Deletion of the mitochondrial chaperone TRAP-1 uncovers global reprogramming of metabolic networks*. **Cell Rep**. 8:671.

4. Other achievements.

More recent experiments expanded the preclinical characterization of Gamitrinib in anticipation of combination anticancer regimens in prostate cancer. In these studies, we performed a high-throughput drug combination screen, and demonstrated that Gamitrinib potently and selectively synergized with small molecule inhibitors of the PI3K/Akt/mTOR pathway currently in clinical trials. The molecular basis for this synergistic effect is under investigation and evidence points to a role of adaptive mitochondrial reprogramming in conferring resistance to PI3K therapy. Conversely, Gamitrinib treatment abolishes the compensatory response of mitochondrial adaptation and restores the sensitivity of tumor cells to PI3K therapy. In xenograft models, the combination of Gamitrinib plus PI3K therapy strongly inhibited tumor growth with minimal systemic or organ toxicity. A new manuscript describing these findings has been submitted for consideration (Ghosh et al, 2014), and is currently under review.

- **What opportunities for training and professional development has the project provided?**
  The present application was not designed to provide a training and professional development environment. Nothing to report.

- **How were the results disseminated to communities of interest?**
  The findings described above were disseminated through publication of two research articles in the peer-reviewed, premiere biomedical literature (Nature Comm; Cell Reports); one oral presentation at a national conference (Keystone Conference on Mitochondrial Dynamics and Physiology, Santa Fe, NM -18/2/2014 – 23/2/2014); and submission for publication of a new manuscript describing the synergy between Gamitrinib and PI3K/Akt/mTOR small molecule antagonists currently in clinical development.

- **What do you plan to do during the next reporting period to accomplish the goals?**
  During the next reporting period, we will pursue the experimental tasks set forth in the SOW of the present application. As a global metabolomics and biomarker signature for the anticancer activity of Gamitrinib has now been validated, we will determine the optimal formulation requirements of Gamitrinib (i), validate an HPLC-based method for the detection of Gamitrinib in plasma (ii), reach a comprehensive pharmacokinetics profile of Gamitrinib administration in vivo (iii), and begin IND-enabling toxicology, toxicokinetics and pharmacodynamics studies of systemic Gamitrinib therapy, in vivo (iv).

4. IMPACT

- **What was the impact on the development of the principal disciplines of the project?** The results outlined above have significant impact for the experimental and medical fields of tumor metabolic reprogramming (i), rewiring of mitochondrial functions in cancer (ii), and opportunities for molecular therapy created by targeting these pathways (iii). Although tumor metabolism is a validated therapeutic target in cancer, the identification and preclinical development of small molecule antagonists of these pathways for cancer therapy have not been widely reported. Our findings that Gamitrinib therapy induces major metabolic defects in tumor cells (i), that these changes provide reproducible biomarkers of anticancer activity in genetic models of prostate cancer (ii), and that targeting these mechanisms results in potent anticancer activity in single agent or combination regimens, in vivo, establish a pivotal, first-in-class proof of concept. As a result of our studies, targeting mitochondrial bioenergetics for cancer therapy is now proven feasible, supported by validated companion biomarkers of metabolic imbalance in immunocompetent tumor models. In terms of drug development, these findings further validate the rationale for the preclinical development of Gamitrinib in anticipation of

human testing as a first-in-humans therapeutic approach to target aberrant tumor metabolic reprogramming in prostate cancer patients.

- **What was the impact on other disciplines?** The results above have also relevance for other experimental fields of biochemistry and molecular biology, advancing our understanding of regulatory mechanisms of bioenergetics. Although the function of oxidative phosphorylation has long been established, the identification of a key role of Hsp90 chaperone-directed protein folding as a prerequisite for cellular respiration has not been previously appreciated. Second, our identification of a mitochondrial Hsp90 proteome that oversees virtually every organelle function suggests that Hsp90-directed protein folding plays a pivotal role in maintaining mitochondrial homeostasis. Finally, our data demonstrate that mitochondrial bioenergetics is not a static process, but continuously undergoes flexible modulation and adaptation in response to cellular stress, relying on transcriptional regulation of oxidative phosphorylation and glycolysis effectors, as reflected by the compensatory and adaptive phenotypes of TRAP-1 knockout mice.

- **What was the impact on technology transfer?** Nothing to report.

- **What was the impact on society beyond science and technology?** Nothing to report.

5. CHANGES/PROBLEMS.

- **Changes in approach**. We do not anticipate any changes in approach for the further preclinical development of Gamitrinib. The results reported above provide an ideal mechanistic foundation for the further characterization of Gamitrinib's drug formulation, HPLC-based detection in plasma, pharmacokinetics, and toxicology.

- **Actual or anticipated problems or delays and actions or plans to resolve them**. We do not anticipate problems or delays in carrying out and successfully accomplish the milestones set forth in the year 2 of the SOW for the present application.

- **Changes that had a significant impact on expenditures**. None reported.

- **Significant changes in use or care of human subjects, vertebrate animals, biohazards, and/or select agents**. None reported.

6. PRODUCTS

- **Publications, conference papers, and presentations**

Journal Publications

  - Chae et al. (2013) *Landscape of the mitochondrial Hsp90 proteome in tumors*. **Nature Commun**. 4:2139. Acknowledgement of federal support –specific for this award (no)
  - Lisanti et al (2014) *Deletion of the mitochondrial chaperone TRAP-1 uncovers global reprogramming of metabolic networks*. **Cell Reports**. 8:671. Acknowledgement of federal support –specific for this award (yes)
  - Ghosh et al (2014) Adaptive mitochondrial reprogramming confers resistance to PI3K therapy. Manuscript submitted for publication. Acknowledgement of federal support – specific for this award (yes)

Other publications, conference papers, and presentations

  - Keystone Conference on Mitochondrial Dynamics and Physiology, Santa Fe, NM -18/2/2014 – 23/2/2014. Oral presentation: Dario C. Altieri, M.D.

Websites or other Internet sites. Nothing to report

Technologies or techniques. Nothing to report

Inventions, patent applications, and/or licenses. Nothing to report

Other products

  - Research material: Generation of TRAP-1 knockout mice

7. PARTICIPANTS & OTHER COLLABORATING ORGANIZATIONS

- What individuals have worked on the project

Name:	Dario C. Altieri, M.D.
Project Role:	Principal Investigator
Researcher Identifier (e.g. ORCID ID):	
Nearest person month worked:	2
Contribution to Project:	Dr. Altieri coordinated and oversaw all of the studies of preclinical development of Gamitrinib, metabolomics screening and characterization of a biomarker signature of Gamitrinib anticancer activity in TRAMP mice

Funding Support:	In addition to the present award, these studies are also supported by NIH NCI CA78810 and CA140043. There is no scientific or budgetary overlap between any grants listed.

Name:	Young Chan Chae, Ph.D.
Project Role:	Postdoctoral Fellow
Researcher Identifier (e.g. ORCID ID):	
Nearest person month worked:	6
Contribution to Project:	Dr. Chae participated in the characterization of Gamitrinib regulation of mitochondrial bioenergetics, metabolomics profiling, and identification of a mitochondrial Hsp90 proteome
Funding Support:	In addition to the present award, these studies are also supported by NIH NCI CA78810 and CA140043. There is no scientific or budgetary overlap between any grants listed.

Name:	Sofia Lisanti, Ph.D.
Project Role:	Postdoctoral Fellow
Researcher Identifier (e.g. ORCID ID):	
Nearest person month worked:	3
Contribution to Project:	Dr. Lisanti carried out the generation and characterization of TRAP-1 knockout mice, including metabolic reprogramming, defective mitochondrial respiration and switch to aerobic glycolysis in vivo.
Funding Support:	In addition to the present award, these studies are also supported by NIH NCI CA78810 and CA140043. There is no scientific or budgetary overlap between any grants listed.

Name:	Jagadish C. Ghosh, Ph.D.
Project Role:	Postdoctoral Fellow
Researcher Identifier (e.g. ORCID ID):	
Nearest person month worked:	2
Contribution to Project:	Dr. Ghosh conducted a high-throughput drug screening to characterize the preclinical activity of Gamitrinib in combination with other molecular therapies, and the role of mitochondria in adaptive reprogramming to small molecule PI3K antagonists.
Funding Support:	In addition to the present award, these studies are also supported by NIH NCI CA78810 and CA140043. There is no scientific or budgetary overlap between any grants listed.

- **Has there been a change in the active other support of the PD/PI(s) or senior/key personnel since the last reporting period?** Nothing to report.

- **What other organizations were involved as partners?**
  Organization: Thomas Jefferson University, Department Nuclear Medicine
  Location: Philadelphia, PA
  Contribution: Collaboration on the ^{18}F-FDG-PET studies on WT and TRAP-1 knockout mice.

  Organization: University of Pennsylvania Veterinary School
  Location: Philadelphia, PA
  Contribution: Collaboration on histologic characterization of TRAP-1 knockout mice.

8. SPECIAL REPORTING REQUIREMENTS

Nothing to report

9. APPENDICES

Reprints of published journal articles immediately relevant to the proposed studies.

- Chae et al. (2013) *Landscape of the mitochondrial Hsp90 proteome in tumors*. **Nature Commun**. 4:2139.
- Lisanti et al (2014) *Deletion of the mitochondrial chaperone TRAP-1 uncovers global reprogramming of metabolic networks*. **Cell Reports**. 8:671

nature COMMUNICATIONS

ARTICLE

Received 5 Apr 2013 | Accepted 13 Jun 2013 | Published 10 Jul 2013

DOI: 10.1038/ncomms3139

Landscape of the mitochondrial Hsp90 metabolome in tumours

Young Chan Chae[1], Alessia Angelin[2], Sofia Lisanti[1], Andrew V. Kossenkov[3], Kaye D. Speicher[3], Huan Wang[3], James F. Powers[4], Arthur S. Tischler[4], Karel Pacak[5], Stephanie Fliedner[5], Ryan D. Michalek[6], Edward D. Karoly[6], Douglas C. Wallace[2], Lucia R. Languino[1,7], David W. Speicher[3] & Dario C. Altieri[1,3]

Reprogramming of tumour cell metabolism contributes to disease progression and resistance to therapy, but how this process is regulated on the molecular level is unclear. Here we report that heat shock protein 90-directed protein folding in mitochondria controls central metabolic networks in tumour cells, including the electron transport chain, citric acid cycle, fatty acid oxidation, amino acid synthesis and cellular redox status. Specifically, mitochondrial heat shock protein 90, but not cytosolic heat shock protein 90, binds and stabilizes the electron transport chain Complex II subunit succinate dehydrogenase-B, maintaining cellular respiration under low-nutrient conditions, and contributing to hypoxia-inducible factor-1α-mediated tumorigenesis in patients carrying succinate dehydrogenase-B mutations. Thus, heat shock protein 90-directed proteostasis in mitochondria regulates tumour cell metabolism, and may provide a tractable target for cancer therapy.

[1] Prostate Cancer Discovery and Development Program, The Wistar Institute, Philadelphia, Pennsylvania 19104, USA. [2] Center for Mitochondrial and Epigenomic Medicine, Children's Hospital of Philadelphia, Philadelphia, Pennsylvania 19104, USA. [3] Molecular and Cellular Oncogenesis Program and Center for Systems and Computational Biology, The Wistar Institute, Philadelphia, Pennsylvania 19104, USA. [4] Department of Pathology, Tufts Medical Center, Boston, Massachusetts 02111, USA. [5] Program in Reproductive and Adult Endocrinology, Eunice Kennedy Shriver National Institute of Child Health and Human Development, National Institutes of Health, Bethesda, Maryland 20892, USA. [6] Metabolon, Inc, Durham, North Carolina 27713, USA. [7] Department of Cancer Biology, Kimmel Cancer Center, Thomas Jefferson University, Philadelphia, Pennsylvania 19107, USA. Correspondence and requests for materials should be addressed to D.C.A. (email: daltieri@wistar.org).

Reprogramming of tumour cell metabolism[1] is increasingly recognized as a multifaceted disease driver, enhancing biomass expansion[2], and promoting various mechanisms of oncogenic signalling[3]. Although these processes have been mostly studied in the context of aerobic glycolysis, the so-called Warburg effect[3], there is evidence that mitochondria continue to have an important role in tumour metabolism[4,5], and organelle-driven oxidative phosphorylation has been associated with tumorigenic potential[6], drug resistance[7,8] and enhanced tumour cell survival[9]. Harnessing these pathways may open new prospects for cancer therapy[10], but the regulators of mitochondrial homeostasis in tumours have remained largely elusive, and their potential suitability as drug candidates is unknown.

With a complex, multi-compartment topology, dependence on import of nuclear-encoded proteins and production of protein-modifying reactive oxygen species (ROS), mitochondria must tightly control their protein folding environment[11]. This is indispensable to maintain metabolic output[2], ensure organelle integrity[12] and prevent the consequences of an unfolded protein response, which may result in cell death[13]. Buffering mitochondrial proteotoxic stress, especially in the protein-dense and energy-producing organelle matrix[14], relies on adaptive responses mediated by molecular chaperones and AAA proteases[15], and dysregulation of these mechanisms has been linked to human diseases, including neurodegeneration and cancer[14].

In this context, a pool of ATPase-directed molecular chaperones, including heat shock protein 90 (Hsp90)[16] and its related homologue, TNF receptor-associate protein-1 (TRAP-1)[17] localize to the mitochondria, almost exclusively in tumour cells[18]. The molecular requirements for the selective accumulation of these chaperones in tumour mitochondria have not been completely elucidated. However, there is evidence that both Hsp90 and TRAP-1 form overlapping complexes with mitochondrial proteins, including cyclophilin D (CypD), a component of the permeability transition pore and control their folding[19]. Accordingly, inhibition of Hsp90 and TRAP-1 chaperone activity selectively in mitochondria triggered acute organelle dysfunction[20], defective hexokinase II (HK-II)-dependent[2] ATP production[21], and anticancer activity in preclinical tumour models, *in vivo*[19].

In this study, we examined the role of Hsp90-directed mitochondrial protein folding on cellular homeostasis. Using combined proteomics and metabolomics approaches, we found that mitochondrial Hsp90 and TRAP-1 are global regulators of tumour metabolic reprogramming, including oxidative phosphorylation, and are required for disease maintenance.

Results

Identification of a mitochondrial Hsp90 proteome. We began this study by setting up a preliminary proteomics screen to identify regulators of mitochondrial protein homeostasis, or proteostasis, in tumours. For these experiments, we used non-cytotoxic concentrations of Gamitrinib (GA mitochondrial matrix inhibitor), a mitochondrial-targeted, small molecule ATPase antagonist that inhibits the chaperone activity of both Hsp90 and TRAP-1 in tumours[20].

Treatment of glioblastoma LN229 cells with non-cytotoxic concentrations of Gamitrinib[21] caused the accumulation of aggregated and misfolded proteins, characterized by resistance to detergent solubilization (Supplementary Fig. S1). Preliminary mass spectrometry analysis of selected bands showing higher intensities with Gamitrinib treatment identified 96 mitochondrial proteins (Supplementary Data 1). Forty-four of these proteins based on spectral counts were elevated by more than threefold after Gamitrinib treatment, indicating a requirement of Hsp90 for their folding. Although gel-based comparison (Supplementary Fig. S1) provides high detection sensitivity for specific bands, individual bands are not single proteins, and slight differences in band excision between control and Gamitrinib treatment can produce artificial differences. To minimize this concern, this experiment focused primarily on band differences at the 2% CHAPS condition, where protein complexity was the lowest, but not necessarily where the largest fold change occurred. To independently validate these initial results, we next performed unbiased proteomics studies using stable isotope labelling by amino acids in culture (SILAC) of control or Gamitrinib-treated cells. Of the original 44 proteins of the mitochondrial Hsp90 proteome identified by 1D mass spectrometry, 33 were independently confirmed for response to Gamitrinib in SILAC experiments (Fig. 1a). Of the remaining 11 proteins, 7 were below adequate detection levels for SILAC quantification, and 4 did not show significant changes.

These verified mitochondrial Hsp90-regulated proteins (Fig. 1a and Supplementary Table S1) comprised the following: transcription factors *TFB1M* and *TFB2M* involved in organelle gene expression[22] and glucose homeostasis[23]; ribosomal proteins (*MRPLs, MTG1* and *ERAL1*) associated with RNA translation[24–26]; regulators of purine biosynthesis and the methyl cycle (*MTHFD2*)[27]; and effectors of oxidative phosphorylation[2], including *SDHB*, *IDH3G, NDUFS3*, *PDHB* and *MDH2* (ref. 28) (Fig. 1b). Mitochondrial proteins participating in redox status and detoxification pathways (*PRDX6, POLDIP2, CYB5R1* and *ETHE1*)[29–31] were also identified in the mitochondrial Hsp90 proteome (Fig. 1b).

Mitochondrial Hsp90 regulation of tumour metabolism. The impact of a mitochondrial Hsp90 proteome (Fig. 1b) on cellular homeostasis was next investigated. For these experiments, we quantified the level of 301 individual metabolites in prostate adenocarcinoma PC3 cells treated with non-cytotoxic concentrations of Gamitrinib[21] or, alternatively, silenced for expression of TRAP-1 by small interfering RNA (siRNA)[21]. Both approaches produced global defects in tumour cell metabolism (Supplementary Data 2). Consistent with a requirement of Hsp90 for oxidative phosphorylation (Fig. 1b), Gamitrinib-treated cells exhibited aberrant accumulation of citric acid cycle metabolites, succinate, fumarate and malate (Fig. 2a). This was associated with altered glutaminolysis (elevation in glutamine and α-ketoglutarate) (Supplementary Fig. S2) and deregulated fatty acid metabolism (Fig. 2b), leading to higher levels of palmitate and linoleate, increased long chain fatty acid transport into mitochondria (elevation of palmitoylcarnitine and stearoylcarnitine), and excess lipid oxidation (accumulation of the ketone body 3-hydroxybutyrate (Supplementary Fig. S3). Mitochondrial Hsp90-targeted cells also showed increased AMP/ATP ratio (Supplementary Fig. S3), indicative of cellular starvation, and consistent with the loss of ATP production, phosphorylation of the energy sensor, AMP-activated kinase (AMPK), and inhibition of mammalian target of Rapamycin complex (mTORC1) observed in response to Gamitrinib[21].

Targeting mitochondrial Hsp90s impaired the catabolism of branched-chain amino acids, with accumulation of valine, isoleucine and leucine (Fig. 2c), and decreased levels of branched-chain amino acid catabolites, isobutyryl-carnitine, succinylcarnitine, 2-methylbutyryl-carnitine and isovaleryl-carnitine (Fig. 2c, Supplementary Fig. S4). This was associated with defects in redox status (Fig. 2d), cholesterol homeostasis (Fig. 2e) and purine nucleotide metabolism (Fig. 2f), resulting in higher levels of cholesterol metabolites associated with lipid

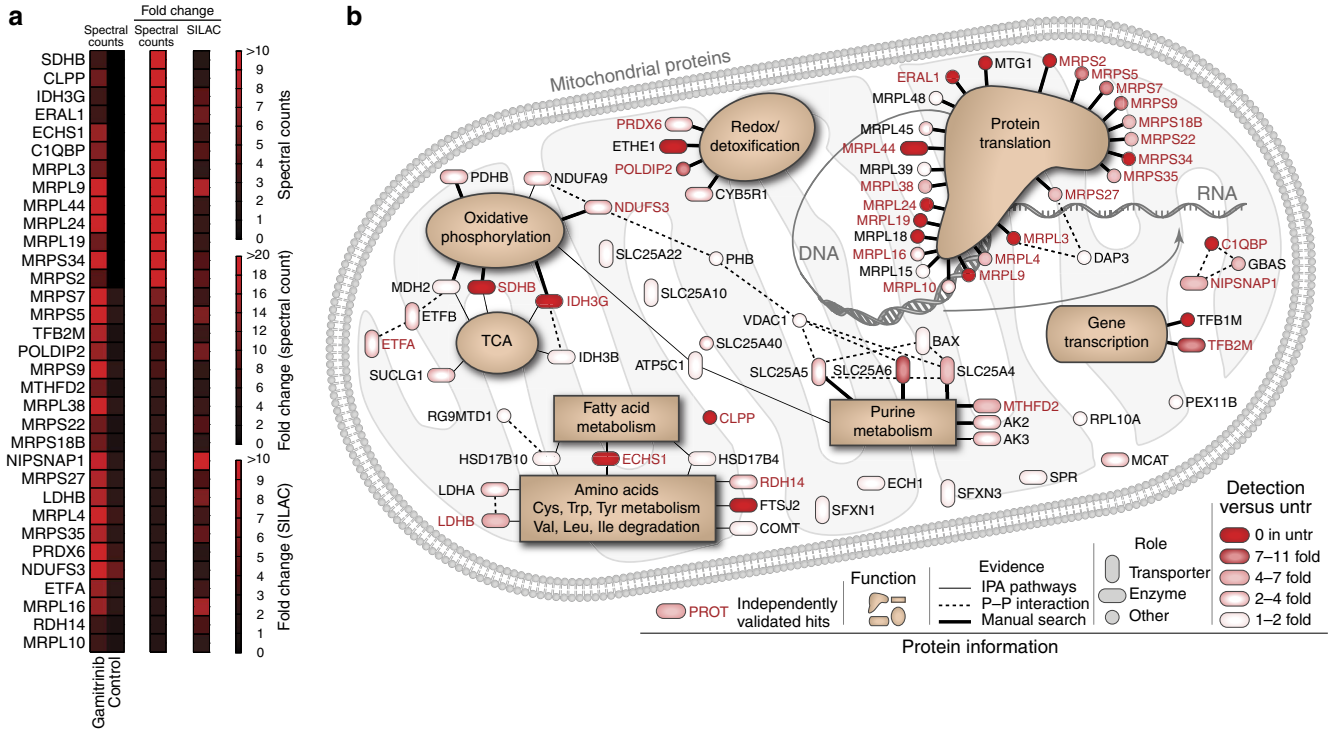

Figure 1 | Mitochondrial Hsp90 proteome. (**a**) LN229 cells were treated with vehicle (Control) or non-cytotoxic concentrations of mitochondrial-targeted Hsp90 inhibitor, Gamitrinib, and detergent-insoluble mitochondrial proteins were identified by one dimensional mass spectrometry (spectral counts), or, alternatively, by SILAC technology. The heat map quantifies changes in protein solubility (>3-fold cutoff) between the treatments assessed using the two independent proteomics approaches. (**b**) Schematic representation of the mitochondrial Hsp90 proteome. Proteins are annotated with functions based on literature search and information from Ingenuity software, which was also used to determine known direct protein–protein interactions. All proteins are colour coded to reflect the magnitude of difference in detection between treated and untreated (untr) samples. Proteins marked in 'red' exhibited a >3-fold change difference after Gamitrinib treatment compared with control, and were independently confirmed by both one dimensional mass spectrometry and SILAC technology.

peroxidation, ROS-dependent allantoin generation (Fig. 2f, Supplementary Fig. S5), and increased oxidized glutathione, cysteine-glutathione disulphide and the glutathione catabolic product, 5-oxoproline (Supplementary Fig. S6). Increased ROS production under these conditions may result from dysfunctional mitochondrial metabolism (see above), and/or increased nitric oxide generation from arginine, a possibility suggested by the accumulation of citrulline under these conditions (Fig. 2g, Supplementary Fig. S7).

Overall, Gamitrinib treatment produced more extensive changes in the tumour metabolome, compared with siRNA silencing of TRAP-1 (Fig. 2 and Supplementary Figs S2–S7). This may reflect incomplete TRAP-1 knockdown by siRNA, or, alternatively, compensatory mechanisms provided by mitochondrial Hsp90, which is inhibited by Gamitrinib, but not by TRAP-1 knockdown. As a control, treatment of PC3 cells with 17-allylamino 17-demethoxygeldanamycin (17-AAG), which inhibits Hsp90 in the cytosol, but not mitochondria[20], or transfection of a control, non-targeting siRNA, had minimal effects on metabolic pathways (Supplementary Figs S2–7). In previous experiments, addition of the triphenylphosphonium 'mitochondriotropic' moiety, alone or in the presence of 17-AAG, had no effect on mitochondrial function[20].

Mechanism of mitochondrial Hsp90 control of tumour metabolism. To elucidate how mitochondrial Hsp90s regulate tumour bioenergetics, we next focused on SDHB, the iron–sulphur subunit of ETC Complex II[32], which required Hsp90s for proper folding (Fig. 1a,b, Supplementary Table S1, Supplementary Data 1), and functional activity (Supplementary Fig. S2). Treatment of tumour cells with Gamitrinib caused insolubility of Complex II over a range of detergent concentrations (Fig. 3a and Supplementary Fig. S8a). In contrast, mitochondrial proteins comprising other ETC Complexes (I, IV, III and V) were minimally affected (Fig. 3a). Immune complexes precipitated from mitochondrial fractions of tumour cells with two independent antibodies to SDHB, but not control IgG, contained TRAP-1, *in vivo* (Supplementary Fig. S8b). In addition, immunoprecipitated SDHB associated with recombinant TRAP-1, *in vitro* (Supplementary Fig. S8c), demonstrating that these two proteins interact in tumour mitochondria. Suggestive of a chaperone-'client protein' recognition[33], this interaction was required to preserve SDHB stability, as Gamitrinib treatment (Fig. 3b), or siRNA silencing of TRAP-1 (Supplementary Fig. S8d) caused SDHB degradation in tumour cells (Fig. 3c).

We next asked whether a TRAP-1–SDHB complex was important during cellular stress. In control experiments, exposure of tumour cells to concentrations >50 μM of the oxidative agent, hydrogen peroxide (H_2O_2), reduced SDHB levels (Fig. 3d). siRNA silencing of TRAP-1 exacerbated this response and induced nearly complete loss of SDHB expression at lower H_2O_2 concentrations (Fig. 3d). As a control, the expression of the flavoprotein subunit of Complex II, SDHA[28], was not affected (Fig. 3d). Functionally, treatment of tumour cells with Gamitrinib inhibited Complex II activity in a concentration-dependent manner, whereas 17-AAG had no effect (Fig. 3e). Reciprocally, addition of recombinant TRAP-1

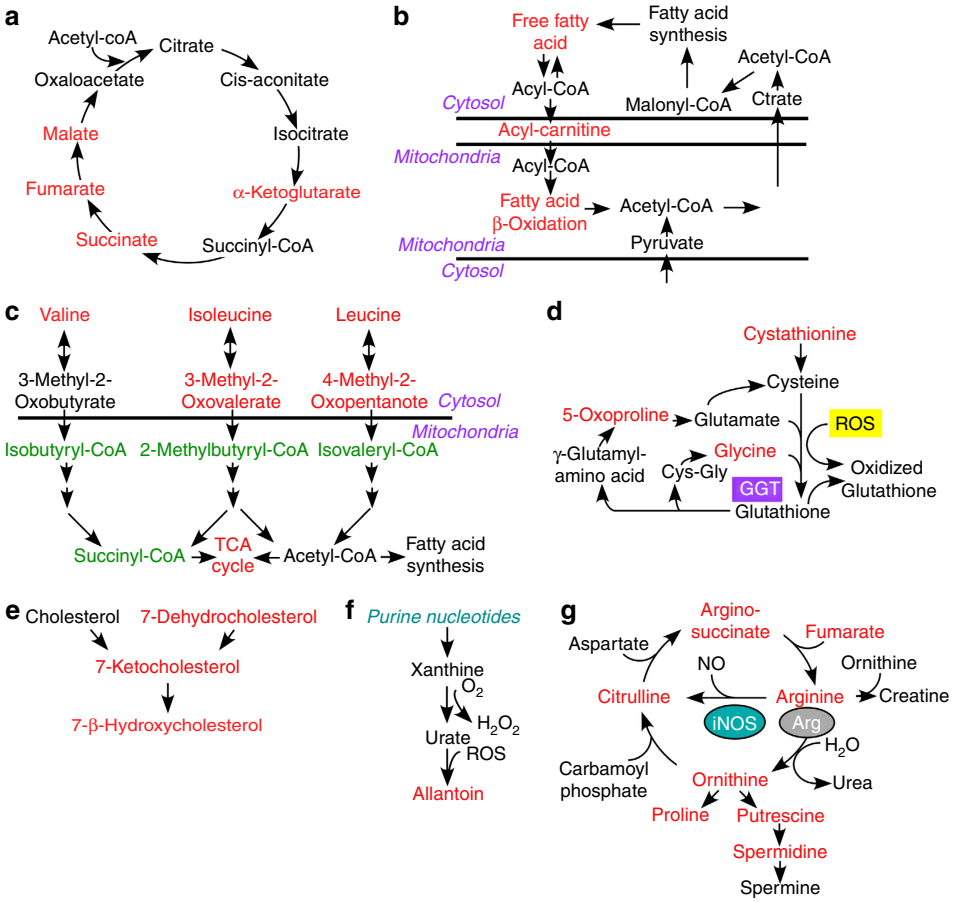

Figure 2 | Mitochondrial Hsp90 control of tumour cell metabolism. PC3 cells were transfected with control non-targeting siRNA or TRAP-1-directed siRNA, or, alternatively, treated with non-cytotoxic concentrations of 17-AAG (5 μM) or Gamitrinib (2.5–5 μM), and analysed for changes in expression of 301 individual metabolites by mass spectrometry. The complete summary of metabolic changes induced by targeting mitochondrial Hsp90s is presented in Supplementary Data 2. The experiment was carried out once with five independent replicates per condition tested. The metabolic pathways affected under these conditions are depicted as follows: (**a**) citric acid cycle; (**b**) fatty acid oxidation; (**c**) branched-chain amino acid catabolism; (**d**) redox status; (**e**) cholesterol metabolism; (**f**) purine nucleotide metabolism; and (**g**) arginine metabolism. Significant ($P<0.05$) changes in metabolite levels within each group (Ctrl versus TRAP-1 siRNA or vehicle versus Gamitrinib) are indicated in red (increase) or green (decrease) using Welch's two-sample *t*-test ($n=5$).

to SDHB immuno-affinity isolated from mitochondrial extracts enhanced Complex II activity in a concentration-dependent manner, *in vitro* (Fig. 3f).

Mitochondrial Hsp90 regulation of bioenergetics stress. The results above have suggested that Hsp90-directed protein folding preserves the stability and function of SDHB in tumour cells. To determine whether this mechanism regulates oxidative phosphorylation, we next quantified the respiration rates of tumour cells in real time. At the same concentrations that induce SDHB misfolding (Fig. 3a), and impaired mitochondrial metabolism (Figs 1,2), Gamitrinib inhibited the oxygen consumption rate (OCR) in prostate PC3 cancer (Fig. 3g,h, Supplementary Fig. S9a), or glioblastoma LN229 (Supplementary Fig. S9b–d) cells, in a concentration-dependent manner. 17-AAG had no effect on OCR (Fig. 3g,h, Supplementary Fig. 9). siRNA knockdown of TRAP-1 in PC3 (Fig. 3i,j, Supplementary Fig. S10a), or LN229 (Supplementary Fig. S10b–d) cells, partially attenuated the inhibition of OCR mediated by Gamitrinib, compared with control transfectants. In contrast, transfection of tumour cells with non-targeting siRNA had no effect on OCR, with or without Gamitrinib (Fig. 3i,j, Supplementary Fig. S10a–d). The partial reduction in the respiratory capacity and SDHB inhibition produced by Gamitrinib when added after siRNA silencing of TRAP-1, as compared with the near complete inhibition observed when Gamitrinib is added without prior siRNA to TRAP-1, may reflect a compensatory protective response by the mitochondria as a result of the extended partial TRAP-1 inhibition produced by siRNA knockdown of TRAP-1, potentially involving organelle Hsp90.

Most tumours undergo metabolic reprogramming, and utilize aerobic glycolysis as their main energy source[3]. Therefore, we asked whether oxidative phosphorylation enabled by Hsp90-directed protein folding was important for tumour maintenance. Tumour cells transfected with control siRNA and maintained in abundant nutrients (10 mM glucose) exhibited normal cellular respiration (Fig. 4a,b, Supplementary Fig. S10e). This response was increased at lower glucose concentrations (1 mM), suggestive of a compensatory mechanism that elevates ATP output by oxidative phosphorylation during nutrient deprivation (Fig. 4a,b, Supplementary Fig. S10e). Under these experimental conditions, siRNA knockdown of TRAP-1 abolished the compensatory increase in OCR at limiting glucose concentrations (1 mM), whereas cellular respiration in 10 mM glucose was minimally affected (Fig. 4a,b, Supplementary Fig. S10e).

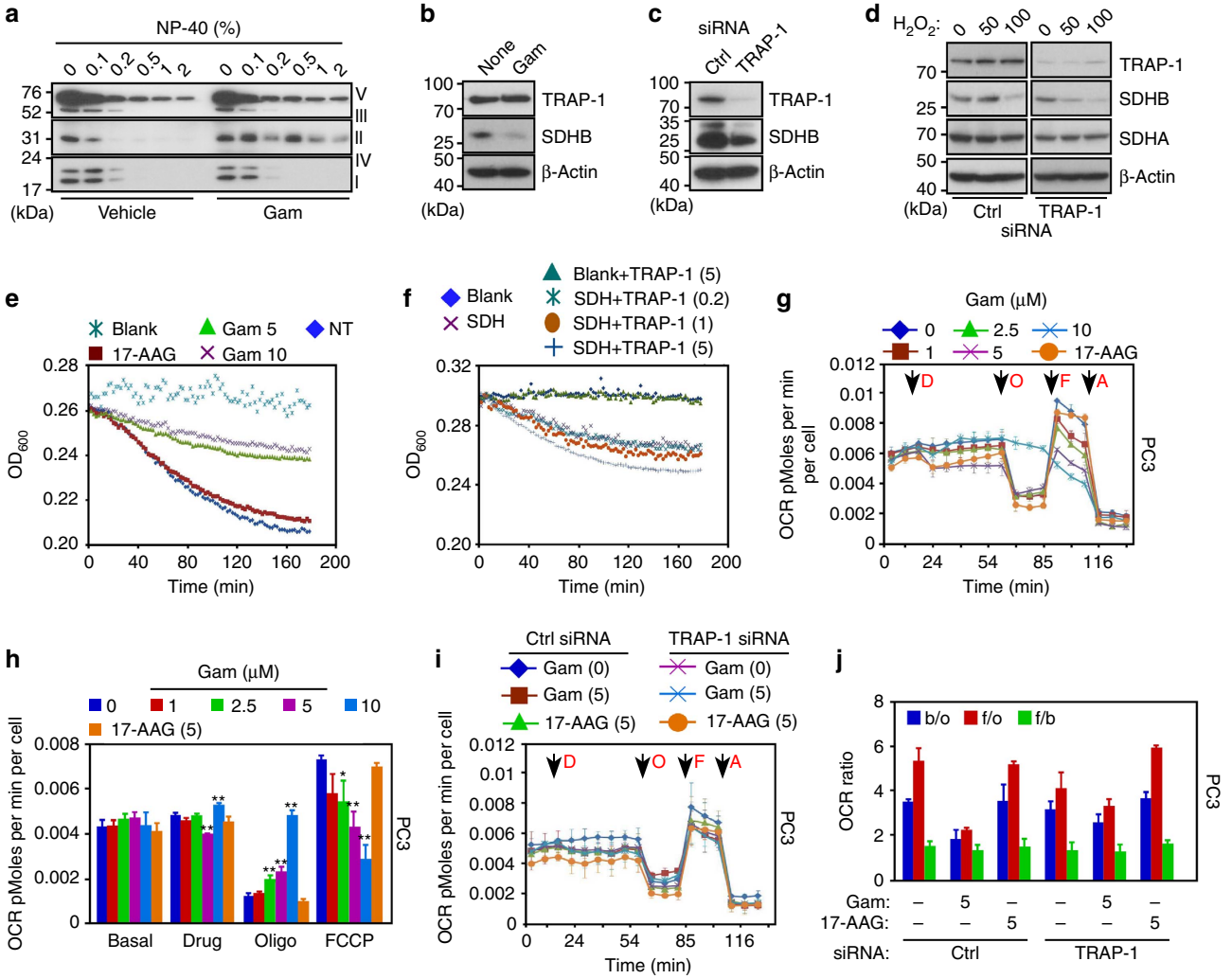

Figure 3 | Mitochondrial Hsp90 regulation of cellular respiration. (**a**) PC3 cells were treated with vehicle or Gamitrinib (Gam), solubilized in the indicated increasing concentrations of detergent (NP-40), and insoluble proteins were analysed by western blotting with an antibody cocktail to the OXPHOS complex. (**b**,**c**) PC3 cells were treated with Gamitrinib (**b**) or transfected with control non-targeting siRNA (Ctrl) or TRAP-1-directed siRNA (**c**), and analysed by western blotting. None, untreated. (**d**) PC3 cells were transfected as in (**c**), treated with the indicated increasing concentrations of H_2O_2 (μM), and analysed by western blotting. (**e**) PC3 cells were treated with the indicated concentrations of Gamitrinib (Gam, μM) or 17-AAG (10 μM) and analysed for SDHB activity at the indicated time intervals. NT, not treated. (**f**) Endogenous Complex II (SDH) was immunoprecipitated from PC3 cells, and analysed for SDHB activity in the presence of increasing concentrations of recombinant TRAP-1 (μM). Data for panels (**e**,**f**) are from representative experiments out of at least two independent determinations. (**g**) PC3 cells were treated with 17-AAG (5 μM) or the indicated increasing concentrations of Gamitrinib (Gam, μM) and the OCR was measured in real time under basal condition and in response to the indicated inhibitors. Arrows indicate the time of drug addition: D, Gamitrinib (Gam) or 17-AAG; O, oligomicyin (1.25 μM); F, FCCP (0.4 μM); A, antimycin (1.8 μM). (**h**) The OCR was normalized by the number of cells, and the extra-mitochondrial respiration after addition of antimycin was subtracted as background. $^*P<0.05$; $^{**}P<0.01$ versus control sample at each state (two-sided unpaired *t*-test). (**i**) PC3 cells were transfected with control (Ctrl) siRNA or TRAP-1-directed siRNA, treated with Gamitrinib (Gam, μM) or 17-AAG and analysed for OCR as in (**g**). (**j**) Quantification of OCR ratio between: b/o, basal condition (before any addition) and after oligomycin addition; f/o, after FCCP and oligomycin addition; f/b, after FCCP addition and basal condition in PC3 cells transfected with control siRNA (Ctrl) or TRAP-1-directed siRNA. $^*P<0.05$; $^{**}P<0.01$ (two-sided unpaired *t*-test). For all OCR experiments, data are representative of two independent experiments carried out in triplicate, mean ± s.d.

In reciprocal experiments, we transfected a control plasmid or TRAP-1 cDNA in normal NIH3T3 fibroblasts (Fig. 4c), which have low endogenous levels of mitochondrial Hsp90 and TRAP-1 (ref. 18). NIH3T3 fibroblasts transfected with control cDNA exhibited reduced ATP production (Fig. 4c), and phosphorylation of AMPK (Fig. 4d) at limiting glucose concentrations, consistent with cellular starvation. In contrast, transfection of TRAP-1 restored ATP production (Fig. 4c), and reduced AMPK phosphorylation (Fig. 4d) at low glucose concentrations.

Role of mitochondrial Hsp90s in SDH-mutant tumours. These experiments suggest that Hsp90 and TRAP-1 control multiple mitochondrial pathways of bioenergetics, and their role in oxidative phosphorylation may support energy production under conditions of nutrient deprivation. To test the implications of this model for tumour cell survival, we next targeted ETC Complex II function using pharmacological inhibitors. Treatment of tumour cells with the Complex II inhibitor, thenoyltrifluoroacetone (TTFA), but not 3-nitropropionic acid, increased the expression

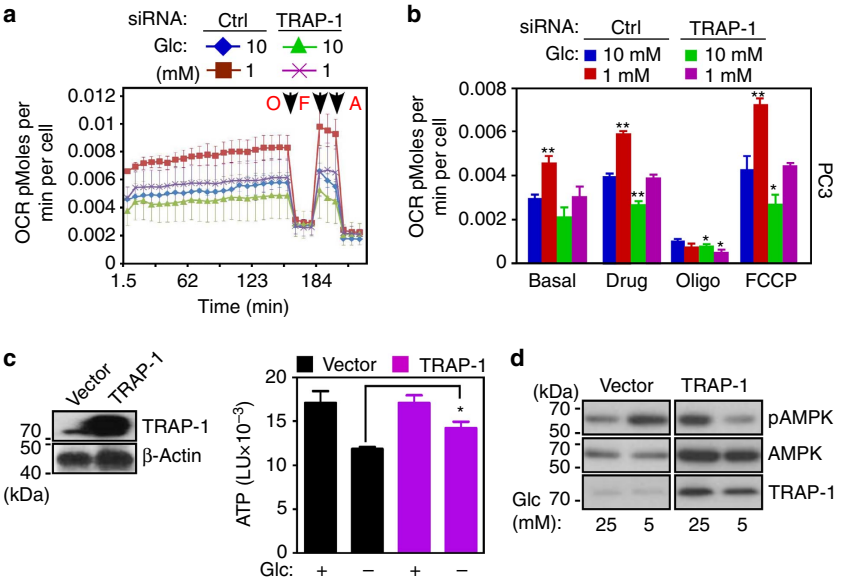

Figure 4 | Mitochondrial Hsp90 regulation of stress bioenergetics. (**a**) PC3 cells were transfected with control, non-targeting siRNA (Ctrl) or TRAP-1-directed siRNA and maintained in 1 or 10 mM glucose (Glc) for 3 h before analysis of OCR. Arrows indicate the time of drug addition: O, oligomicyin (1.25 μM); F, FCCP (0.4 μM); A, antimycin (1.8 μM). (**b**) OCR in **a** was quantified in siRNA-transfected cells in different glucose (Glc) concentrations. Data for panels (**a**,**b**) data are representative of two independent experiments carried out in triplicate, mean ± s.d. $^{*}P<0.05$; $^{**}P<0.01$ versus control sample at each state (two-sided unpaired *t*-test). (**c**) Normal NIH3T3 fibroblasts were transfected with control vector or TRAP-1 cDNA and analysed by western blotting (left) or ATP production in the presence (+) or absence (−) of glucose (Glc, 25 mM) (*right*). $^{*}P=0.03$ (two-sided unpaired *t*-test). (**d**) NIH3T3 fibroblasts were transfected as in (**c**), incubated with the indicated concentrations of glucose (Glc, mM), and analysed by western blotting. p, phosphorylated.

of hypoxia-inducible factor-1α (HIF-1α) (Fig. 5a), an oncogenic transcription factor implicated in adaptive responses to cellular stress[34]. Inhibition of mitochondrial Hsp90s with Gamitrinib (Fig. 5b), or siRNA silencing of TRAP-1 (Fig. 5c), was insufficient, alone, to modulate HIF-1α levels, whereas both treatments strongly enhanced TTFA induction of HIF-1α in tumour cells (Fig. 5b,c). In parallel experiments, tumour cells exposed to hypoxia exhibited increased recruitment of Hsp90 to mitochondria, compared with cytosol (Fig. 5d,e), and this response was reversed by HIF-1α silencing by siRNA (Fig. 5f,g). The mitochondrial pool of HK-II was also increased under hypoxic conditions (Fig. 5d,e), and this response was also abolished by siRNA knockdown of HIF-1α (Fig. 5f,g). In contrast, normoxic conditions (Fig. 5d,e), or transfection of tumour cells with non-targeting siRNA (Fig. 5f,g) had no effect.

Mutations in Complex II[35], including SDHB[36], have been linked to hereditary or sporadic pheochromocytoma (PCC)[37], and paraganglioma (PGL)[38], potentially through a mechanism of HIF-1α-dependent tumorigenesis[39]. Consistent with HIF-1α-dependent accumulation of Hsp90 to mitochondria after Complex II inhibition (Fig. 5e,g), TRAP-1 was strongly expressed in PCC/PGL samples carrying *SDHB* and *SDHD* mutations, compared with tumours with mutations in *RET*, *NF1* and *VHL*, or of unknown genotype (Fig. 5h,i). Functionally, PCC/PGL tumours with Complex II mutations and high levels of TRAP-1 (Fig. 5j) were more sensitive to Gamitrinib-mediated killing, *in vitro* (Fig. 5j), suggesting a compensatory pro-survival role of mitochondrial Hsp90s in transformed cells with defective oxidative phosphorylation[39].

Discussion

In this study, we have identified mitochondrial Hsp90s[18] as global regulators of tumour cell metabolism, including oxidative phosphorylation and redox networks. This pathway hinges on chaperone-directed protein folding in mitochondria[15], and affects a discrete Hsp90/TRAP-1[18] proteome intercalated in multiple, fundamental pathways of cellular homeostasis. This mechanism may be ideally suited to buffer the risk of proteotoxic stress in transformed cells with high biosynthetic needs[19], preserve organelle integrity against CypD-dependent apoptosis[20] and maintain multiple sources of energy production, including HK-II-dependent glycolysis[21], and oxidative phosphorylation (this study), especially under stress conditions of hypoxia and nutrient deprivation.

The considerable interest in aerobic glycolysis[3] as a central feature of tumour metabolic reprogramming[1], together with the signalling role of oncogenes in these responses[40], have brought into question the function of mitochondrial bioenergetics, and in particular oxidative phosphorylation, in tumour maintenance[28]. However, recent studies have suggested that mitochondrial oxidative phosphorylation continues to remain critical for tumour cells[6], favouring resistance to therapy[7,8] and promoting cell survival[9]. The data presented here provide a mechanistic framework in support of these observations, and identify Hsp90/TRAP-1-directed protein folding in mitochondria[18] as a key requirement of oxidative phosphorylation in tumours. This involved the formation of physical complex(es) between Hsp90/TRAP-1 and the iron–sulphur subunit of mitochondrial ETC Complex II, SDHB[32], preserving its folding, stability and enzymatic function under oxidative stress. Functionally, Hsp90/TRAP-1 regulation of SDHB maintained energy production under conditions of low nutrients and hypoxia, which are hallmarks of tumour growth, *in vivo*[41], and dampened biochemical signals of cellular starvation that are typically associated with tumour suppression[42].

SDHB[32] has attracted attention as a gene mutated in certain human neuroendocrine tumours[36]. The molecular requirements

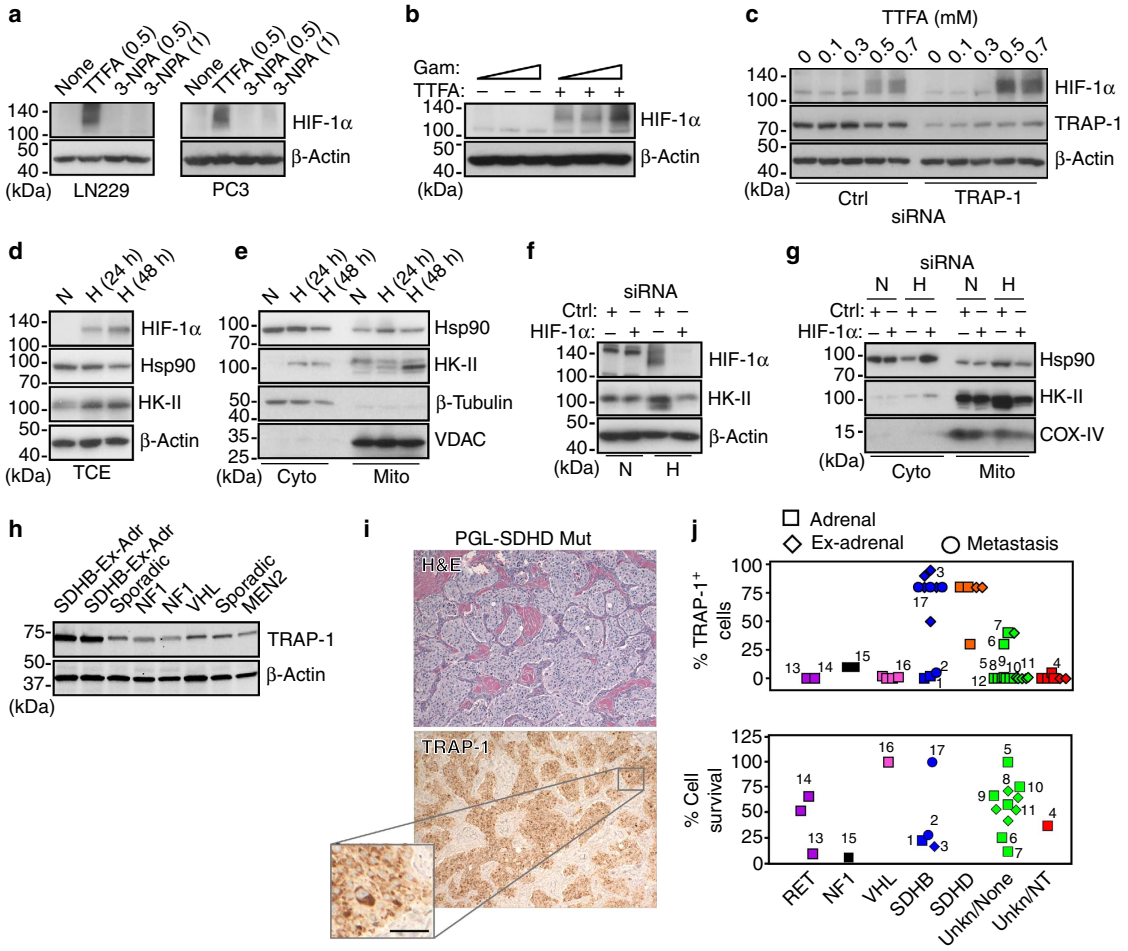

Figure 5 | TRAP-1–SDHB complex regulates HIF-1α-directed tumorigenesis. (**a**) The indicated tumour cell types (LN229 or PC3 cells) were treated with the various concentrations (mM) of the SDHB inhibitors, TTFA or 3-nitropropionic acid (3-NPA) and analysed by western blotting. (**b**) PC3 cells were treated with increasing concentrations of Gamitrinib (Gam, 0, 2.5, 5 μM) in the absence (−) or presence (+) of TTFA (0.3 mM) and analysed by western blotting. (**c**) LN229 cells were transfected with control siRNA (Ctrl) or TRAP-1-directed siRNA and analysed by western blotting in the presence of the indicated increasing concentrations of TTFA. (**d**,**e**) PC3 cells were maintained under conditions of hypoxia (H, 0.5% O_2, 5% CO_2, and 94% N_2 for 24 h) or normoxia (N), and analysed by western blotting in total cell extracts (TCE) (**d**), or fractionated cytosolic (Cyto) or mitochondrial (Mito) extracts (**e**). VDAC or β-tubulin was used as a mitochondrial or cytosolic marker, respectively. (**f**) PC3 cells were transfected with control siRNA (Ctrl) or HIF-1α-directed siRNA, maintained in normoxia (N) or hypoxia (H) conditions, and analysed by western blotting. (**g**) PC3 cells were transfected and treated as in (**f**), and isolated cytosolic (Cyto) or mitochondrial (Mito) fractions were analysed by western blotting. COX-IV was used as a mitochondrial marker. (**h**) Patient-derived tissue samples of PCC/PGL were analysed by western blotting. The mutational status of each tumour is indicated. Ex-Adr, extra-adrenal localization. (**i**) A tissue sample of extra-adrenal PGL with *SDHD* mutation, showing a typical nest-like ('Zellballen') growth pattern was stained with hematoxylin/eosin (H&E, top) or TRAP-1 (bottom), by immunohistochemistry. Scale bar, 50 μm. (**j**) Quantification of immunohistochemical expression of TRAP-1 in PCC/PGL cases with the indicated mutational status (top). Cells from the various tumour samples were maintained in culture and analysed for killing by Gamitrinib (10 μM for 2 weeks) (bottom) measured by counts of tyrosine hydroxylase-positive cells counted in an area defined by a randomly placed 22 × 22 mm^2 coverslips in 35 mm round culture dishes. Each point represents a single tumour. Paired samples of the same tumour were available in 12 instances and are indicated by matching numbers. Data are from a representative experiment.

of how these mutations contribute to malignancy are still being worked out[36], but one consequence of pharmacological or genetic inactivation of SDHB observed here was an increased recruitment of Hsp90 to mitochondria[18]. This pathway required HIF-1α, which is deregulated in SDHB-mutant tumours, and may potentially contribute to disease maintenance[39]. The increased accumulation of mitochondrial Hsp90s under these conditions may help compensate for the impaired oxidative phosphorylation resulting from defective SDHB function[36], enhancing organelle integrity against CypD-mediated permeability transition[18] and energy production via HK-II-directed glycolysis[21]. Consistent with this model, SDHB-mutant tumour cells were more sensitive to Gamitrinib-mediated killing than other neuroendocrine malignancies, suggesting that Hsp90-directed protein folding in mitochondria provides an adaptive and potentially 'addictive' survival factor for these cells.

There is now intense interest in pursuing aberrant tumour cell metabolism for cancer therapeutics[10]. However, inhibitors that can safely target these pathways in tumours, as opposed to normal tissues, especially with respect to oxidative phosphorylation[7,8], have not been clearly identified[43]. As a mitochondrial-directed Hsp90 inhibitor[20], Gamitrinib may be ideally suited to function as a general antagonist of tumour cell metabolism. Supported by the differential targeting of

tumour, as opposed to normal mitochondria[18], and a favourable safety profile in preclinical models[20], Gamitrinib inhibition of mitochondrial Hsp90s may simultaneously disable metabolic and survival adaptive networks in genetically heterogeneous tumours.

Methods

Antibodies and reagents. The following antibodies to succinate dehydrogenase complex subunit B (SDHB, 1:500, Abcam), succinate dehydrogenase complex subunit A (SDHA, 1:3000, Abcam), HK-II (1:1000, Cell Signaling), Cox-IV (1:1000, Cell Signaling), hypoxia-inducible factor-1α (HIF-1α, 1:500, Cell Signaling), Hsp90 (1:1000, BD Biosciences), Thr172-phosphorylated AMPKα (1:1000, Cell Signaling), AMPKα (1:1000, Cell Signaling), TRAP-1 (1:1000, BD Biosciences), and β-actin (1:5000, Sigma-Aldrich) were used. A total oxidative phosphorylation antibody cocktail (1:500, Mitoscience) directed against the 20-kDa subunit of Complex I (20 kDa), cytochrome C oxidase subunit II of Complex IV (22 kDa), SDHB subunit of Complex II (30 kDa), core 2 of Complex III (~ 50 kDa) and F1α (ATP synthase) of Complex V (~ 60 kDa) was used. The complete chemical synthesis, HPLC profile, and mass spectrometry of mitochondrial-targeted small molecule Hsp90 antagonist, Gamitrinib has been reported[20]. The Gamitrinib variant containing triphenylphosphonium as a mitochondrial-targeting moiety[20] was used in this study. Non-mitochondrially directed Hsp90 inhibitor, 17-AAG was obtained from LC-Laboratories. Oligomycin, carbonyl cyanide p-trifluoromethoxyphenylhydrazone (FCCP), antimycin A, 3-nitropropionic acid and (TTFA) were obtained from Sigma-Aldrich.

Transfections. For gene knockdown experiments, tumour cells were transfected using control, non-targeting siRNA pool (Dharmacon, cat. no. D-001810) or specific ON-Target SMARTpool siRNAs to TRAP-1 (Dharmacon, cat. no. L-010104) or HIF-1α (Dharmacon, cat. no. L-004018). The various siRNAs were transfected at 10–30 nM using Oligofectamine (Invitrogen). Transfection of plasmid DNA was carried out with Lipofectamine (Invitrogen), as described[20].

Subcellular fractionation. Mitochondrial fractions were isolated from Gamitrinib-treated LN229 cells (0–20 μM for 5 h) using an ApoAlert cell fractionation kit (Clontech), as described[20]. Briefly, LN229 cells or PC3 cells were mechanically disrupted by 70 strokes with a Dounce homogenizer in isolation buffer containing 1 mM DTT plus protease inhibitor cocktail. Cell debris was removed by centrifugation at 700 *g* for 10 min. The supernatant was further centrifuged at 10,000 *g* for 25 min, and supernatants or mitochondrial pellets were processed for further analysis.

Mitochondrial protein folding. Mitochondrial fractions were isolated from vehicle- or Gamitrinib-treated LN229 cells (5 μM for 12 h), and suspended in equal volume of mitochondrial fractionation buffer containing increasing concentrations of CHAPS (0, 0.05, 0.1, 0.2, 0.5, 1 or 2%). Samples were incubated for 20 min on ice and detergent-insoluble protein aggregates were recovered by centrifugation (20,000 *g*) for 20 min. Pelleted proteins were separated by SDS-gel electrophoresis and visualized by silver staining (Sigma-Aldrich).

Proteomics studies. To identify mitochondrial proteins that require organelle Hsp90s for proper folding and/or activity (mitochondrial Hsp90 proteome), individual silver-stained bands isolated from mitochondrial fractions of vehicle or Gamitrinib-treated LN229 cells were analysed by 1D MS (see Supplementary Methods). As an independent experimental approach, global proteomics analysis of vehicle or Gamitrinib-treated LN229 cells was carried out by SILAC technology (see Supplementary Methods). Changes in the expression of 301 metabolites were determined by ultrahigh performance liquid chromatography/mass spectroscopy and gas chromatography/mass spectroscopy in PC3 cells treated with vehicle or Gamitrinib (2.5, 5 μM), non-mitochondrial-targeted 17-AAG (5 μM), or alternatively, transfected with control non-targeting or TRAP-1-directed siRNA (see Supplementary Methods).

Purification of TRAP-1 proteins. NIH3T3 cells were transfected with human TRAP-1-Myc plasmid cDNA. After 48 h, cells were washed with PBS and lysed in PBS containing 1% TX-100 plus phosphatase inhibitor cocktail (Roche). Lysates were centrifuged at 14,000 *g* for 10 min at 4 °C, and c-Myc-tagged TRAP-1 proteins were isolated by immunoprecipitation with an antibody to c-Myc coupled to agarose beads (Sigma-Aldrich). Samples were then washed five times with lysis buffer, and TRAP-1-myc was eluted from the immune complex with 100 μg ml^{-1} c-Myc peptide (Sigma-Aldrich) in PBS. To eliminate free c-Myc peptide and further enrich eluted TRAP-1-containing material, samples were purified with centrifugal filter (30 K, Millipore).

SDH activity assay. Tumour cells were analysed for SDH complex activity as reduction of the dye 2,6-dichlorophenolindophenol, which recycles the substrate ubiquinone using Complex II enzyme activity. Briefly, mitochondria isolated from PC3 or LN229 cells were lysed in enzyme assay buffer containing 1% *N*-dodecyl-β-D-maltopyranoside plus protease inhibitors (Roche) for 1 h at 4 °C under constant agitation. After centrifugation at 15,000 *g* for 20 min at 4 °C, supernatants were loaded on anti-Complex II antibody-coated 96-well plates, and incubated with increasing concentrations of recombinant TRAP-1 for 2 h. Enzyme activity was determined from SDH-dependent reduction of dye 2,6-dichlorophenolindophenol, and quantified as changes in absorbance at 600 nm for 3 h at 2 min intervals using a plate reader (Beckman Coulter).

Cellular respiration. OCRs were assayed using the Extracellular Flux System 24 Instrument (Seahorse Bioscience, Billerica, MD). PC3 or LN229 cells were grown in standard media and after trypsinization and re-suspension in growth media, 25,000 cells were plated in each well of a Seahorse XF24 cell culture plate (100 μl volume). After 4-h incubation to allow the cells to adhere to the plate, an additional 150 μl of media was added to each well, and the cells were grown for 24 h at 37 °C with 5% CO_2. The media was then exchanged with unbuffered DMEM XF assay media (Seahorse Bioscience) supplemented with 2 mM glutaMAX, 1 mM sodium pyruvate and 5 mM glucose (pH 7.4 at 37 °C), and equilibrated for 30 min at 37 °C and ~0.04% CO_2 before the experiment. Cellular oxygen consumption was monitored in basal condition (before any addition) and after addition of oligomycin (1.25 μM), FCCP (0.4 μM) and antimycin (1.8 μM), all dissolved in DMSO. The three drugs were injected into the XF24 sequentially, and the OCRs measured using the extracellular flux analyser with three cycles of mixing (150 s), waiting (120 s) and measuring (210 s). This cycle was repeated following each injection[44]. To test the effect of mitochondrial Hsp90s on cellular respiration, PC3 or LN229 cells were treated with non-cytotoxic concentrations of Gamitrinib (0–10 μM) or 17-AAG (2.5–5 μM) and continuously analysed for OCR changes. Alternatively, cells were transfected with control or TRAP-1-directed siRNA and analysed after 24–36 h.

Patient samples. All experiments involving patient-derived material were approved by the Tufts Medical Center Institutional Review Board following informed consent. A series of genetically characterized PCC/PGL with documented mutations of major susceptibility genes ($n = 10$, *SDHB*; 6 *SDHD*; 4 *VHL;* 3 *RET*; 2 *NF1*), apparently sporadic PCC/PGL ($n = 22$) and normal human adrenal medulla was examined in this study. All of the tumours with *VHL*, *RET* or *NF1* mutations were intra-adrenal, while 10/13 with *SDHB,* 3/6 with *SDHD*, and 10/25 with no known mutations were extra-adrenal. Two of the extra-adrenal tumours with *SDHD* mutations were in the head or neck and the remainder retroperitoneal. For four of the tumours with *SDHB* mutations, tissue was available only from metastatic sites. One *SDHB*-mutated tumour was an adrenal bed recurrence of a primary malignancy that had given rise to metastases. All of the other specimens were primary tumours.

Statistical analysis. Data were analysed using the two-sided unpaired *t*-tests using a GraphPad software package (Prism 4.0) for Windows. Data are expressed as mean ± s.d. or mean ± s.e.m. of multiple independent experiments. A *P*-value of < 0.05 was considered as statistically significant. For pair-wise comparisons in metabolite screening studies, the Welch's t-tests, Wilcoxon's rank sum tests or ANOVA were performed. For classification studies, random forest analyses were performed. Statistical analyses are performed with the program 'R' http://cran.r-project.org/.

References

1. Kroemer, G. & Pouyssegur, J. Tumor cell metabolism: cancer's Achilles' Heel. *Cancer Cell* **13,** 472–482 (2008).
2. Vander Heiden, M. G., Cantley, L. C. & Thompson, C. B. Understanding the Warburg effect: the metabolic requirements of cell proliferation. *Science* **324,** 1029–1033 (2009).
3. Koppenol, W. H., Bounds, P. L. & Dang, C. V. Otto Warburg's contributions to current concepts of cancer metabolism. *Nat. Rev. Cancer.* **11,** 325–337 (2011).
4. Gao, P. *et al.* c-Myc suppression of miR-23a/b enhances mitochondrial glutaminase expression and glutamine metabolism. *Nature* **458,** 762–765 (2009).
5. Matoba, S. *et al.* p53 regulates mitochondrial respiration. *Science* **312,** 1650–1653 (2006).
6. Weinberg, F. *et al.* Mitochondrial metabolism and ROS generation are essential for Kras-mediated tumorigenicity. *Proc. Natl Acad. Sci. USA* **107,** 8788–8793 (2010).
7. Haq, R. *et al.* Oncogenic BRAF regulates oxidative metabolism via PGC1alpha and MITF. *Cancer Cell* **23,** 302–315 (2013).
8. Caro, P. *et al.* Metabolic signatures uncover distinct targets in molecular subsets of diffuse large B cell lymphoma. *Cancer Cell* **22,** 547–560 (2012).
9. Vazquez, F. *et al.* PGC1alpha expression defines a subset of human melanoma tumors with increased mitochondrial capacity and resistance to oxidative stress. *Cancer Cell* **23,** 287–301 (2013).
10. Wang, J. B. *et al.* Targeting mitochondrial glutaminase activity inhibits oncogenic transformation. *Cancer Cell* **18,** 207–219 (2010).

11. Haynes, C. M. & Ron, D. The mitochondrial UPR—protecting organelle protein homeostasis. *J. Cell. Sci.* **123,** 3849–3855 (2010).
12. Green, D. R. & Kroemer, G. The pathophysiology of mitochondrial cell death. *Science* **305,** 626–629 (2004).
13. Tabas, I. & Ron, D. Integrating the mechanisms of apoptosis induced by endoplasmic reticulum stress. *Nat. Cell. Biol.* **13,** 184–190 (2011).
14. Wallace, D. C. A mitochondrial paradigm of metabolic and degenerative diseases, aging and cancer: A dawn for evolutionary medicine. *Annu. Rev. Genet* **39,** 359–407 (2005).
15. Baker, B. M. & Haynes, C. M. Mitochondrial protein quality control during biogenesis and aging. *Trends Biochem. Sci.* **36,** 254–261 (2011).
16. Taipale, M., Jarosz, D. F. & Lindquist, S. HSP90 at the hub of protein homeostasis: emerging mechanistic insights. *Nat. Rev. Mol. Cell. Biol.* **11,** 515–528 (2010).
17. Leskovar, A., Wegele, H., Werbeck, N. D., Buchner, J. & Reinstein, J. The ATPase cycle of the mitochondrial Hsp90 analog Trap1. *J. Biol. Chem.* **283,** 11677–11688 (2008).
18. Kang, B. H. *et al.* Regulation of tumor cell mitochondrial homeostasis by an organelle-specific Hsp90 chaperone network. *Cell* **131,** 257–270 (2007).
19. Siegelin, M. D. *et al.* Exploiting the mitochondrial unfolded protein response for cancer therapy in mice and human cells. *J. Clin. Invest* **121,** 1349–1360 (2011).
20. Kang, B. H. *et al.* Combinatorial drug design targeting multiple cancer signaling networks controlled by mitochondrial Hsp90. *J. Clin. Invest.* **119,** 454–464 (2009).
21. Chae, Y. C. *et al.* Control of tumor bioenergetics and survival stress signaling by mitochondrial HSP90s. *Cancer Cell* **22,** 331–344 (2012).
22. Litonin, D. *et al.* Human mitochondrial transcription revisited: only TFAM and TFB2M are required for transcription of the mitochondrial genes in vitro. *J. Biol. Chem* **285,** 18129–18133 (2010).
23. Koeck, T. *et al.* A common variant in TFB1M is associated with reduced insulin secretion and increased future risk of type 2 diabetes. *Cell. Metab.* **13,** 80–91 (2011).
24. Barrientos, A. *et al.* MTG1 codes for a conserved protein required for mitochondrial translation. *Mol. Biol. Cell* **14,** 2292–2302 (2003).
25. Christian, B. E. & Spremulli, L. L. Mechanism of protein biosynthesis in mammalian mitochondria. *Biochim. Biophys. Acta* **1819,** 1035–1054 (2012).
26. Uchiumi, T. *et al.* ERAL1 is associated with mitochondrial ribosome and elimination of ERAL1 leads to mitochondrial dysfunction and growth retardation. *Nucleic Acids Res.* **38,** 5554–5568 (2010).
27. Pike, S. T., Rajendra, R., Artzt, K. & Appling, D. R. Mitochondrial C1-tetrahydrofolate synthase (MTHFD1L) supports the flow of mitochondrial one-carbon units into the methyl cycle in embryos. *J. Biol. Chem.* **285,** 4612–4620 (2010).
28. Wallace, D. C. Mitochondria and cancer. *Nat. Rev. Cancer.* **12,** 685–698 (2012).
29. Eismann, T. *et al.* Peroxiredoxin-6 protects against mitochondrial dysfunction and liver injury during ischemia-reperfusion in mice. *Am. J. Physiol. Gastrointest. Liver Physiol.* **296,** G266–G274 (2009).
30. Lyle, A. N. *et al.* Poldip2, a novel regulator of Nox4 and cytoskeletal integrity in vascular smooth muscle cells. *Circ. Res* **105,** 249–259 (2009).
31. Tiranti, V. *et al.* Loss of ETHE1, a mitochondrial dioxygenase, causes fatal sulfide toxicity in ethylmalonic encephalopathy. *Nat. Med* **15,** 200–205 (2009).
32. Yankovskaya, V. *et al.* Architecture of succinate dehydrogenase and reactive oxygen species generation. *Science* **299,** 700–704 (2003).
33. Taipale, M. *et al.* Quantitative analysis of HSP90-client interactions reveals principles of substrate recognition. *Cell* **150,** 987–1001 (2012).
34. Shay, J. E. & Celeste Simon, M. Hypoxia-inducible factors: crosstalk between inflammation and metabolism. *Semin. Cell Dev. Biol.* **23,** 389–394 (2012).
35. Neumann, H. P. *et al.* Germ-line mutations in nonsyndromic pheochromocytoma. *N. Engl. J. Med.* **346,** 1459–1466 (2002).
36. King, A., Selak, M. A. & Gottlieb, E. Succinate dehydrogenase and fumarate hydratase: linking mitochondrial dysfunction and cancer. *Oncogene* **25,** 4675–4682 (2006).
37. Astuti, D. *et al.* Gene mutations in the succinate dehydrogenase subunit SDHB cause susceptibility to familial pheochromocytoma and to familial paraganglioma. *Am. J. Hum. Genet.* **69,** 49–54 (2001).
38. Gimenez-Roqueplo, A. P. & Tischler, A. S. Pheochromocytoma and paraganglioma: progress on all fronts. *Endocr. Pathol.* **23,** 1–3 (2012).
39. Selak, M. A. *et al.* Succinate links TCA cycle dysfunction to oncogenesis by inhibiting HIF-alpha prolyl hydroxylase. *Cancer Cell* **7,** 77–85 (2005).
40. Ward, P. S. & Thompson, C. B. Metabolic reprogramming: a cancer hallmark even Warburg did not anticipate. *Cancer Cell* **21,** 297–308 (2012).
41. Laderoute, K. R. *et al.* 5′-AMP-activated protein kinase (AMPK) is induced by low-oxygen and glucose deprivation conditions found in solid-tumor microenvironments. *Mol. Cell. Biol.* **26,** 5336–5347 (2006).
42. Mihaylova, M. M. & Shaw, R. J. The AMPK signalling pathway coordinates cell growth, autophagy and metabolism. *Nat. Cell. Biol.* **13,** 1016–1023 (2011).
43. Cheong, H., Lu, C., Lindsten, T. & Thompson, C. B. Therapeutic targets in cancer cell metabolism and autophagy. *Nat. Biotechnol.* **30,** 671–678 (2012).
44. Wu, M. *et al.* Multiparameter metabolic analysis reveals a close link between attenuated mitochondrial bioenergetic function and enhanced glycolysis dependency in human tumor cells. *Am. J. Physiol. Cell Physiol.* **292,** C125–C136 (2007).

Acknowledgements

We gratefully acknowledge the assistance of The Wistar Institute Proteomics Core for performing LC-MS/MS analyses, Tony Chang-Wong for assistance in computational processing of proteomics data, and Sira Sriswasdi for preparing heat maps. This work was supported by the PheoPara Alliance, National Institutes of Health (NIH) Grants CA140043, CA78810, HL54131 and CA118005 to DCA, NS021328 to DCW and Department of Defense grant PR100171 to AST. Support for Core Facilities utilized in this study was provided by Cancer Center Support Grant (CCSG) CA010815 to The Wistar Institute.

Author contributions

Y.C.C., A.A., A.S.T., R.D.M., D.C.W., L.R.L., D.W.S. and D.C.A. designed research; Y.C.C., A.A., K.D.S., H.W., J.F.P. and E.D.K. performed research; S.L., K.P., S.F. and R.D.M. contributed new reagents/analytical tools; Y.C.C., A.A., A.S.T., R.D.M., D.C.W., L.R.L., D.W.S. and D.C.A. analysed data, and Y.C.C., A.A., A.S.T., D.C.W., D.W.S. and D.C.A. wrote the paper.

Additional information

Supplementary Information accompanies this paper at http://www.nature.com/naturecommunications

Competing financial interests: The authors declare no competing financial interests.

Reprints and permission information is available online at http://npg.nature.com/reprintsandpermissions/

How to cite this article: Chae, Y. C. *et al.* Landscape of the mitochondrial Hsp90 metabolome in tumours. *Nat. Commun.* 4:2139 doi: 10.1038/ncomms3139 (2013).

Cell Reports
Report

Deletion of the Mitochondrial Chaperone TRAP-1 Uncovers Global Reprogramming of Metabolic Networks

Sofia Lisanti,[1,2] Michele Tavecchio,[1,2] Young Chan Chae,[1,2] Qin Liu,[2] Angela K. Brice,[3] Madhukar L. Thakur,[4] Lucia R. Languino,[1,5] and Dario C. Altieri[1,2,*]
[1]Prostate Cancer Discovery and Development Program
[2]Molecular and Cellular Oncogenesis Program
The Wistar Institute, Philadelphia, PA 19104, USA
[3]Department of Pathobiology, School of Veterinary Medicine, University of Pennsylvania, Philadelphia, PA 19104, USA
[4]Department of Radiology
[5]Department of Cancer Biology
Kimmel Cancer Center, Thomas Jefferson University, Philadelphia, PA 19107, USA
*Correspondence: daltieri@wistar.org
http://dx.doi.org/10.1016/j.celrep.2014.06.061

SUMMARY

Reprogramming of metabolic pathways contributes to human disease, especially cancer, but the regulators of this process are unknown. Here, we have generated a mouse knockout for the mitochondrial chaperone TRAP-1, a regulator of bioenergetics in tumors. TRAP-1$^{-/-}$ mice are viable and showed reduced incidence of age-associated pathologies, including obesity, inflammatory tissue degeneration, dysplasia, and spontaneous tumor formation. This was accompanied by global upregulation of oxidative phosphorylation and glycolysis transcriptomes, causing deregulated mitochondrial respiration, oxidative stress, impaired cell proliferation, and a switch to glycolytic metabolism in vivo. These data identify TRAP-1 as a central regulator of mitochondrial bioenergetics, and this pathway could contribute to metabolic rewiring in tumors.

INTRODUCTION

The control of protein folding in subcellular organelles, including mitochondria (Kang et al., 2007), maintains cellular homeostasis (Ellis, 2007) by buffering proteotoxic stress and ensuring flexible adaptation to environmental cues (Balch et al., 2008). In mitochondria, a network of chaperones of the heat shock protein-90 (Hsp90) gene family (Kang et al., 2007), including Hsp90 (Taipale et al., 2010) and its related homolog TNFR-associated protein-1 (TRAP-1) (Lavery et al., 2014), protects against oxidative stress and permeability transition-induced apoptosis (Altieri et al., 2012). This pathway is exploited in cancer, where mitochondrial Hsp90s are dramatically upregulated, compared to normal tissues (Kang et al., 2007).

Recent evidence suggests that mitochondrial Hsp90s may play a more global role in organelle homeostasis. Mechanistically, this involves protein-folding quality control of a discrete mitochondrial Hsp90 proteome, overseeing gene expression, protein translation, redox balance, and a host of metabolic pathways (Chae et al., 2013). In this context, mitochondrial Hsp90s, including TRAP-1, preserve the association of the first enzyme of glycolysis, hexokinase II (HK-II) (Ward and Thompson, 2012) to the organelle outer membrane (Chae et al., 2012), and ensure the folding/stability of the oxidative phosphorylation complex II subunit (Wallace, 2012), succinate dehydrogenase, SDHB (Chae et al., 2013). These functions are important for cellular homeostasis, because targeting TRAP-1 by pharmacologic or genetic approaches irreversibly compromises mitochondrial integrity, impairs both glycolysis (Chae et al., 2012) and oxidative phosphorylation (Chae et al., 2013), and may provide a novel anticancer strategy in humans (Altieri et al., 2012).

However, how TRAP-1 regulation of mitochondrial homeostasis fits with general mechanisms of tumor metabolic reprogramming (Ward and Thompson, 2012) has not been clearly delineated. Known as the "Warburg effect" (Ward and Thompson, 2012), most tumors rewire their energy sources toward aerobic glycolysis and at the expense of mitochondrial respiration (Wallace, 2012). Together with the identification of mutations in oxidative phosphorylation subunits that produce "oncometabolites" (Lu et al., 2012; Turcan et al., 2012) or stabilize oncogenes, such as HIF1α (Selak et al., 2005), this has suggested that mitochondrial bioenergetics has limited (if any) role in cancer (Ward and Thompson, 2012) and may actually function as a "tumor suppressor" (Frezza et al., 2011). In this context, the role of mitochondrial Hsp90s in bioenergetics has become controversial, as conflicting reports in the literature have claimed that TRAP-1 actually inhibits SDHB activity in tumor cells, promoting the accumulation of the oncometabolite, succinate (Sciacovelli et al., 2013), or, conversely, acts as a potential "tumor suppressor" through stimulation of glucose metabolism (Yoshida et al., 2013).

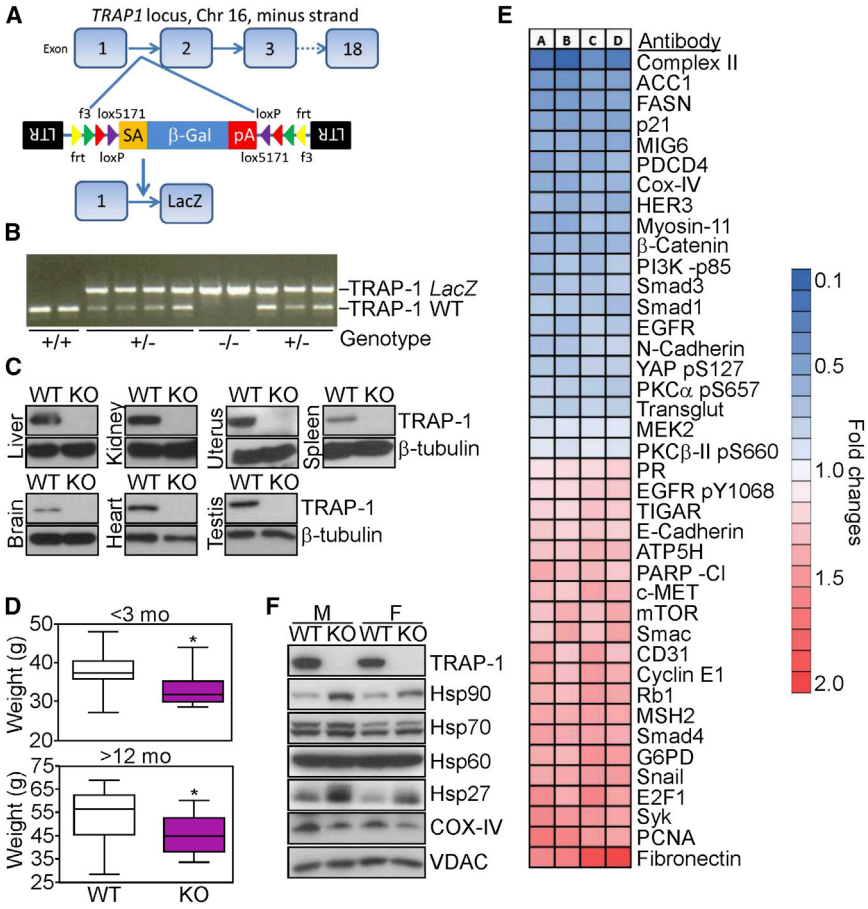

Figure 1. Characterization of TRAP-1$^{-/-}$ Mice

(A) Map of the gene trapping construct and position of the β-galactosidase cassette inserted in the mouse *TRAP-1* locus.

(B) PCR genotyping of TRAP-1 wild-type (WT, +/+), heterozygous (+/−), and homozygous (−/−) mice. The position of WT and LacZ alleles is indicated.

(C) The indicated tissue extracts from WT or TRAP-1 knockout (KO) mice were analyzed by western blotting.

(D) WT or TRAP-1 KO mice were analyzed for changes in body weight at the indicated ages (mo, months). Data are represented as box plots. Ages <3 months (top), WT, n = 16; KO, n = 15; ages >12 months (bottom), WT, n = 16; KO, n = 26. *p = 0.033–0.022.

(E) Heatmap of changes in protein expression and/or phosphorylation in liver extracts isolated from WT or TRAP-1 KO mice (A–C, replicates; D, average), as determined by Reverse Phase Protein Array (RPPA). Blue, downregulated; red, upregulated. Only statistically significant changes ($p < 0.05$) are shown.

(F) Liver extracts from WT or TRAP-1 KO mice were analyzed by western blotting. M, male; F, female.

To clarify mechanisms of metabolic rewiring in mitochondria, and conclusively elucidate the function of mitochondrial Hsp90s in bioenergetics, we have now generated TRAP-1 knockout mice.

RESULTS

Generation of TRAP-1 Knockout Mice

Using gene-trap technology, we obtained mouse ES cells in which a β-galactosidase gene disrupts the TRAP-1 locus on chromosome 16, downstream of exon 1 (Figure 1A). Transfer of TRAP-1-targeted zygotes into C57Bl/6 pseudopregnant recipient mice generated TRAP-1 knockout animals. In genotyping experiments, PCR products of 565 nt, or, conversely, 1,148 nt identified the wild-type (WT) TRAP-1 allele or the β-galactosidase (LacZ)-containing allele, respectively (Figure 1B). TRAP-1 knockout (TRAP-1$^{-/-}$) mice were born viable, fertile, and at expected Mendelian rates for both genders. Analysis of tissues from TRAP-1$^{-/-}$ mice, including liver, kidney, uterus, spleen, brain, heart, and testis confirmed the absence of TRAP-1 protein, compared to WT littermates, by western blotting (Figure 1C). Histologic analysis of 15-month-old TRAP-1$^{-/-}$ mice revealed significantly reduced incidence of multiple age-associated pathologies. Compared to age-matched WT littermates, these included lower body weight (Figure 1D) and organ (liver, spleen) hyperplasia (Figure S1A), decreased chronic inflammatory infiltrates in lung, stomach, pancreas, and small intestine (Figure S1B), lower hepatic lipidosis (Figure S1C), and reduced pancreatic fibrotic degeneration (Figure S1B). Two out of three WT mice examined at this age harbored spontaneous tumors or dysplastic lesions, including bronchoalveolar adenoma, dental dysplasia, and histiocytic sarcoma (Figures S1D–S1H). In contrast, no tumors or dysplasia were detected in age-matched TRAP-1$^{-/-}$ mice. In terms of blood chemistry parameters, a complete blood count was unremarkable between the various animal groups (Figure S1I), whereas TRAP-1$^{-/-}$ mice showed decreased blood levels of glucose (see below) and creatinine, compared to WT animals (Figure S1J).

We next profiled signaling pathways in WT or TRAP-1$^{-/-}$ mice by Reverse Phase Protein Array (RPPA). Consistent with a role of mitochondria in "retrograde" signaling and nuclear gene expression (Butow and Avadhani, 2004), TRAP-1 deletion was associated with general reduction in growth factor receptor activity (MIG6, Her3, EGFR, MEK2, and PI3K), attenuated TGFβ responses (Smad1 and Smad3), modulation of cell-cell and cell-matrix communication (N-cadherin, E-cadherin, β-catenin, transglutaminase, fibronectin), and stimulation of cell-cycle transitions (p21, Rb1, E2F1, cyclin E1, PCNA) (Figure 1E). TRAP-1 deficiency also profoundly affected bioenergetics pathways. Consistent with recent observations (Chae et al., 2013), TRAP-1 loss resulted in significantly reduced levels of mitochondrial complex II subunit, SDHB (Figure 1E). This was associated with reduced expression of fatty acid synthase and mitochondrial complex IV subunit, Cox-IV, upregulation of complex V

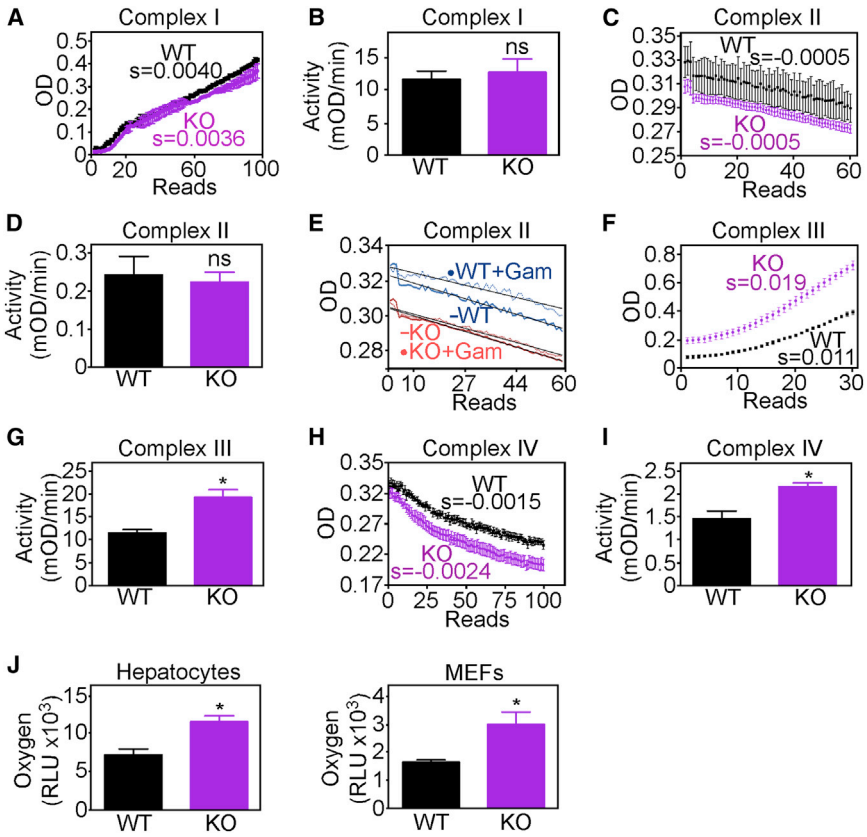

Figure 2. TRAP-1 Regulation of Mitochondrial Oxidative Phosphorylation

(A) Mitochondria isolated from WT or KO hepatocytes were analyzed for complex I activity. The quantification of the slope (s) per each reaction is indicated. Representative experiment.

(B) Quantification of complex-I-specific activity in WT or KO mitochondria. Mean ± SD (n = 3). ns, not significant (p = 0.67).

(C, F, and H) Representative experiments of mitochondrial complex II (C), complex II+III (F), or complex IV (H) activity in mitochondria isolated from WT or KO hepatocytes. The quantification of the slope (s) per each reaction is indicated. Mean ± SD (n = 3).

(D, G, and I) Quantification of mitochondrial complex-II (D), complex-II–III (G), or complex-IV (I) -specific activity in WT or KO hepatocytes. Data per each mitochondrial complex activity were normalized against citrate synthase activity. Mean ± SD (n = 3). ns, not significant (p = 0.66). *p = 0.027–0.033.

(E) Representative experiment of mitochondrial complex II activity in the presence or absence of mitochondrial Hsp90 inhibitor, Gamitrinib (Gam) The slope of individual curves is as follows, WT-Gam, s = −0.0005; WT+Gam, s = −0.0004; KO-Gam, s = −0.0005; KO+Gam, s = −0.0005.

(J) WT or TRAP-1 KO hepatocytes (left) or mouse embryonic fibroblasts (MEFs) (right) were analyzed for oxygen consumption. Data were normalized for cell number by direct counting and cell viability by a fluorescence reporter. Mean ± SD (n = 3) of replicates of a representative experiment. *p = 0.015–0.036.

subunit, ATP5H, and higher levels of the glycolytic enzyme, G6PD (Figure 1E). Decreased Cox-IV expression in TRAP-1$^{-/-}$ mice versus WT samples was confirmed by western blotting (Figure 1F). In addition, liver extracts of TRAP-1$^{-/-}$ mice showed increased recruitment of cytoprotective chaperones Hsp90 (Kang et al., 2007) and Hsp27 to mitochondria, whereas levels of Hsp70, Hsp60, or VDAC were unchanged in WT or TRAP-1$^{-/-}$ mice (Figure 1F).

Requirement of TRAP-1 for Mitochondrial Oxidative Phosphorylation

To examine a role of TRAP-1 in cellular respiration (Chae et al., 2013), we next used purified mitochondria from primary hepatocytes (Figure S2A) and nontransformed mouse embryonic fibroblasts (MEFs) (Figure S2B). In these experiments, citrate synthase-normalized (Figure S2C) mitochondrial complex I activity was not significantly different between WT and TRAP-1$^{-/-}$ mice (Figure 2A), as assessed in three independent mitochondrial preparations (Figure 2B). Complex II activity, which was proposed to be inhibited by TRAP-1 (Sciacovelli et al., 2013), was instead unchanged between the two animal groups (Figures 2C and 2D). In addition, treatment with Gamitrinib, a small molecule antagonist that target TRAP-1/Hsp90 selectively in mitochondria (Chae et al., 2012), inhibited complex II activity in WT mitochondria but had no effect on TRAP-1$^{-/-}$ samples (Figure 2E), consistent with the absence of its target, TRAP-1, in these cells. Conversely, mitochondria isolated from TRAP-1$^{-/-}$ hepatocytes showed significantly increased activity of complex III (Figures 2F and 2G), as well as complex IV (Figures 2H and 2I), compared to WT samples. Consistent with these data, mitochondrial respiration was deregulated in TRAP-1$^{-/-}$ mice and resulted in aberrantly increased oxygen consumption levels, compared to WT cultures (Figure 2J).

The mechanistic underpinning of deregulated cellular respiration in TRAP-1 knockout mice was further investigated. Accordingly, deletion of TRAP-1 resulted in a global compensatory upregulation of an oxidative phosphorylation "transcriptome," with increased expression of virtually every subunit of mitochondrial respiration complexes (Figures S2D–S2H). Compared to WT littermates, this included an average fold increase of 1.31 ± 0.03 (n = 33) for complex I subunits, 1.42 ± 0.081 (n = 4) for complex II, 1.36 ± 0.025 (n = 7) for complex III, and 1.3 ± 0.06 (n = 24) for complex V (Figures S2D–S2F and S2H). Two subunits in complex IV, Cox4i2 and Cox6b2, increased by approximately 4- and 20-fold, respectively, in TRAP-1$^{-/-}$ mice, compared to WT littermates, by array analysis (Figure S2G), as well as quantitative RT-PCR (Figure S2I), resulting in a 2.86 ± 1.34 (n = 15) average fold increase for all complex IV subunits. In contrast, overall mitochondrial DNA content was unchanged in WT or TRAP-1$^{-/-}$ mice (Figure S2J).

Glycolytic Reprogramming in TRAP-1 Knockout Mice

In addition to mitochondrial oxidative phosphorylation, TRAP-1 has been linked to the regulation of glycolysis (Chae et al.,

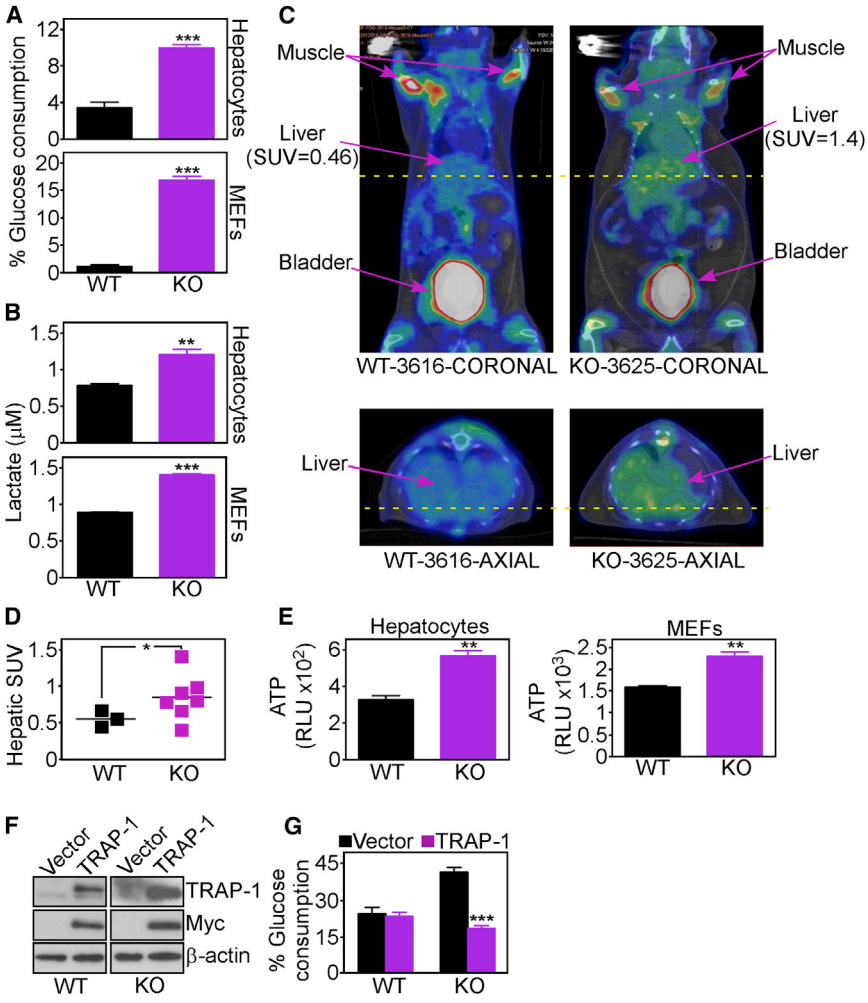

Figure 3. Glycolytic Reprogramming Induced by TRAP-1 Deficiency

(A and B) Mitochondria isolated from WT or TRAP-1 KO hepatocytes (top) or MEFs (bottom) were analyzed for glucose consumption (A) or lactate generation (B). Data were normalized for cell number by direct cell counting and cell viability by a fluorescence reporter. Mean ± SD (n = 3) of replicates. ***p = 0.0001–0.0009; **p = 0.0057.

(C) Whole-body PET/CT coronal (top) or axial (bottom) images of a WT (left) and TRAP-1 KO (right) mouse obtained 1 hr post ^{18}F-FDG injection. Three times greater uptake of radioactivity in the liver of the TRAP-1 KO mouse represents increased glucose consumption. SUV, standardized uptake values.

(D) Quantification of hepatic standardized uptake values (SUVs) of ^{18}F-FDG as determined by PET/CT analysis in WT or TRAP-1 KO mice. Each point corresponds to an individual mouse. *p = 0.03 by Kolmogorov-Smirnov two-sample test.

(E) Mitochondria isolated from WT or TRAP-1 KO hepatocytes (left) or MEFs (right) were analyzed for ATP production. Mean ± SD (n = 3) of replicates. **p = 0.0025.

(F and G) WT or TRAP-1 KO MEFs were transfected with vector or Myc-TRAP-1 cDNA and analyzed by western blotting (F) or glucose consumption (G). Mean ± SD (n = 3) of replicates of a representative experiment. ***p < 0.0001.

2012; Yoshida et al., 2013), and this function was next investigated. Similar to the changes in mitochondrial respiration (Figures S2C–S2G), but in contrast with a recent report (Yoshida et al., 2013), deletion of TRAP-1 resulted in uniformly upregulated expression of a glycolysis "transcriptome" (Figure S3). This involved an average fold increase of 2.36 ± 0.33 (n = 22) for regulators of glycolysis (Figure S3A), 2.28 ± 0.4 (n = 6) for glucose metabolism (Figure S3B), 1.38 ± 0.11 (n = 29) for the TCA cycle (Figure S3C), and 1.61 ± 0.27 (n = 4) for glycogen synthesis (Figure S3D). There was also an average fold increase of 1.78 ± 0.26 (n = 6) for molecules involved in glycogen degradation (Figure S3E), 1.52 ± 0.044 (n = 7) for gluconeogenesis (Figure S3F), and 1.42 ± 0.19 (n = 10) for the pentose phosphate pathway (Figure S3G). Expression of sodium-independent glucose transporters Slc2a2 (Glut2) and Slc2a10 (Glut10) was also increased in TRAP-1$^{-/-}$ hepatocytes, whereas the levels of other glucose transporters, Slc2a4 (Glut4), Slc2a8 (Glut8), and Slc2a9 (Glut9) was unchanged, compared to WT cultures (Figures S4A and S4B). Consistent with these changes, TRAP-1$^{-/-}$ hepatocytes or MEFs dramatically switched their metabolism to aerobic glycolysis compared to WT controls, as reflected by higher glucose consumption (Figure 3A), and increased lactate production (Figure 3B).

To quantify glycolytic reprogramming, in vivo, we next carried out ^{18}F-FDG whole-body positron emission tomography (PET)/computed tomography (CT) scans of WT or TRAP-1$^{-/-}$ mice. In these experiments, TRAP-1$^{-/-}$ mice exhibited a 2- to 3-fold increase in standardized uptake values (SUVs) of the radioactive tracer in the liver, compared to WT littermates, as determined 1 hr post-injection of ^{18}F-FDG (Figures 3C and 3D). Consistent with these data, and together with the increased mitochondrial respiration associated with TRAP-1 deletion (Figure 2), hepatocytes or MEFs isolated from TRAP-1$^{-/-}$ mice exhibited greater ATP production than WT cultures (Figure 3E). Despite their switch to glycolytic metabolism, TRAP-1-deleted cells were as sensitive as WT cultures to apoptosis induced by glucose deprivation (Figure S4C), or treatment with the nonmetabolizable glucose analog, 2-deoxyglucose (2-DG) (Figure S4D), potentially reflecting the higher levels of cytoprotective chaperones Hsp90 and Hsp27 in mitochondria (Figure 1F). To independently validate a role of TRAP-1 in glycolytic reprogramming, we next reconstituted WT or TRAP-1$^{-/-}$ MEFs with control vector or a Myc-TRAP-1 cDNA (Figure 3F). Transient re-expression of TRAP-1 was sufficient to normalize the glycolytic phenotype in these cells, lowering glucose consumption to the levels of WT MEFs (Figure 3G). In contrast, transfection of a TRAP-1 cDNA in WT cultures had no effect on glucose consumption (Figure 3G).

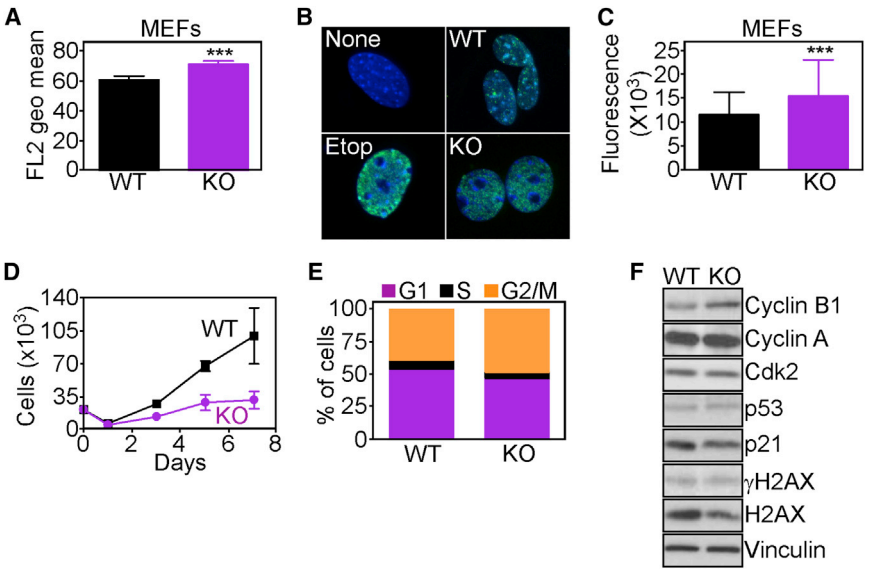

Figure 4. TRAP-1 Deficiency Induces Low-Level Oxidative Damage and Cell-Cycle Defects

(A) WT or TRAP-1 KO MEFs were analyzed for ROS production by flow cytometry. Data are expressed as mean geometric fluorescence. Mean ± SD (n = 5) of replicates of a representative experiment. ***p = 0.0001.

(B and C) WT or TRAP-1 KO MEFs were analyzed for γH2AX reactivity by fluorescence microscopy (B) and quantified as normalized mean fluorescence (C). Mean ± SD (n = 79 for WT and n = 71 for KO cells). Nuclei were stained with DAPI. None, untreated; Etop, etoposide. Magnification, ×60. ***p = 0.0003.

(D) WT or TRAP-1 KO MEFs were analyzed for cell proliferation at the indicated time intervals by direct cell counting. Mean ± SD (n = 3) of replicates. Representative experiment.

(E) WT or TRAP-1 KO MEFs were stained with propidium iodide and analyzed for DNA content by flow cytometry. The percentage of cells in the various cell-cycle transitions is indicated.

(F) WT or TRAP-1 KO MEFs were analyzed by western blotting.

We next asked whether targeting TRAP-1 in tumor cells, which have typically a different bioenergetics profile from normal tissues (Ward and Thompson, 2012), also resulted in metabolic reprogramming. Transfection of prostate adenocarcinoma PC3 cells with four independent TRAP-1-directed siRNAs efficiently silenced TRAP-1 expression (Figure S4E), consistent with previous observations (Chae et al., 2012). Within 6 days of TRAP-1 silencing, these cells already exhibited compensatory increased recruitment of Hsp90 to mitochondria, compared to control transfectants (Figure S4E), thus similar to TRAP-1$^{-/-}$ mice (Figure 1F). Second, we established clones of cervical carcinoma HeLa cells selected for stable small hairpin RNA (shRNA) knockdown of TRAP-1 (Figure S4F). Analysis of these cells also revealed compensatory metabolic reprogramming, with increased oxygen consumption (Figure S4G), and higher ATP production (Figure S4H), compared to shRNA controls, in a response that correlated with the degree of TRAP-1 depletion (Figure S4F).

TRAP-1 Regulation of Oxidative Damage

Deregulated mitochondrial function as observed in TRAP-1$^{-/-}$ cells may result in oxidative stress, and this possibility was next investigated. In these experiments, TRAP-1$^{-/-}$ MEFs exhibited a modest, but significant increased production of reactive oxygen species (ROS), compared to WT cultures (Figures 4A and S4I). TRAP-1 deletion also resulted in consistently higher ROS production in response to increasing oxidative stress (H_2O_2), compared to WT cultures (Figure S4J). Consistent with increased sensitivity to oxidative damage, TRAP-1 KO cells stained positive for markers of a DNA damage response, as reflected by increased reactivity for phosphorylated H2AX (γH2AX) (Figures 4B and 4C). Under these conditions, TRAP-1$^{-/-}$ MEFs exhibited profound defects in cell proliferation compared to WT cultures (Figure 4D), coinciding with cell-cycle arrest at G2/M (Figure 4E), and accumulation of mitotic cyclin B1 (Figure 4F). In contrast, the expression of cyclin A or Cdk2 was unchanged, and p21 levels were reduced in TRAP-1$^{-/-}$ MEFs (Figure 4G), consistent with the data of RPPA profiling (Figure 1D).

DISCUSSION

In this study, we have shown that homozygous deletion of the mitochondrial chaperone TRAP-1 causes global reprogramming of cellular bioenergetics, with compensatory upregulation of oxidative phosphorylation and glycolysis transcriptomes, increased mitochondrial accumulation of cytoprotective chaperones Hsp90 and Hsp27, and a dramatic switch to glycolytic metabolism, in vivo. This is accompanied by reduced incidence of age-associated pathologies, in vivo, including obesity, dysplasia and tumor formation, decreased cell proliferation, and low-level ROS production.

The data presented here refute recent and contradictory claims that TRAP-1 inhibits mitochondrial SDHB-complex II activity (Sciacovelli et al., 2013), or, conversely, promotes glycolysis (Yoshida et al., 2013). These preliminary suggestions were at odd with a large body of literature, in which pharmacologic or genetic targeting of TRAP-1 inhibited mitochondrial respiration (Butler et al., 2012; Chae et al., 2013), impaired mitochondrial quality control (Costa et al., 2013), caused oxidative damage (Butler et al., 2012; Pridgeon et al., 2007), and suppressed ATP production (Agorreta et al., 2014; Chae et al., 2012). Consistent with this model, we found that homozygous deletion of TRAP-1 resulted in decreased SDHB expression, reflecting loss of protein-folding quality control in mitochondria (Chae et al., 2013). Mechanistically, this role of TRAP-1 in organelle protein homeostasis (Chae et al., 2013) emerged here as a critical requirement for mitochondrial bioenergetics. Accordingly, a compensatory upregulation of virtually every effector of oxidative phosphorylation and glycolysis in TRAP-1$^{-/-}$ mice was sufficient to restore complex II activity, increase mitochondrial respiration through

higher activity of complex III and IV (Wallace, 2012), and impart a "pseudo-Warburg" glycolytic phenotype validated in whole-body ^{18}F-FDG PET/CT analysis, in vivo. Together, these findings reinforce a pivotal role of TRAP-1 in maintaining mitochondrial homeostasis and bioenergetics (Chae et al., 2013), not suppressing it (Sciacovelli et al., 2013).

At variance with recent claims of TRAP-1 as a "tumor suppressor" (Yoshida et al., 2013), older TRAP-1$^{-/-}$ mice were instead significantly healthier than their age-matched WT littermates, with significantly reduced obesity, inflammatory and degenerative pathologies, or spontaneous dysplastic lesions, including tumor formation. More work is required to conclusively dissect the observed phenotype. However, increased mitochondrial respiration, as paradoxically induced as compensation for TRAP-1 loss (this study), has been associated with extended lifespan in model organisms (Guarente, 2008), potentially contributing to the increased longevity afforded by calorie restriction (Nisoli et al., 2005). In this context, low levels of mitochondrial respiration-derived ROS, as demonstrated here in TRAP-1$^{-/-}$ mice, may activate "retrograde" gene expression mechanisms of adaptation and cytoprotection (Merksamer et al., 2013) and exert beneficial effects in aging (Schulz et al., 2007). In addition, the combination of a chronic DNA damage response, which opposes malignant transformation (Gorgoulis et al., 2005), and impaired proliferative capacity, as observed here in TRAP-1$^{-/-}$ cells, may further preserve organ integrity during aging.

A pivotal function of TRAP-1 in mitochondrial homeostasis, as reinforced here, suggests that models of extramitochondrial bioenergetics, i.e., aerobic glycolysis (Ward and Thompson, 2012) may not fully recapitulate the complexity of metabolic reprogramming in tumors (Wallace, 2012). In this context, TRAP-1-directed mitochondrial metabolism may be important to support highly energy-demanding traits of tumor cells, for instance, cell invasion (Caino et al., 2013) or cell proliferation (this study), especially under conditions of chronic nutrient deprivation. In parallel, ATP produced under these conditions may blunt tumor suppression mechanisms driven by AMPK activation (Liang and Mills, 2013), escape autophagic cell death (Kimmelman, 2011), and preserve mTOR signaling (Guertin and Sabatini, 2007), all key requirements of tumor progression, in vivo. Consistent with this view, oxidative phosphorylation is being increasingly recognized as a key requirement of aggressive tumor behavior, preserving a cancer stem cell phenotype (Janiszewska et al., 2012), and promoting drug resistant disease (Haq et al., 2013). Together with its broad cytoprotective functions, these properties make TRAP-1 a uniquely attractive therapeutic target in cancer, suitable to disable multiple pathways of bioenergetics, cell survival, and adaptation in genetically heterogeneous tumors (Altieri et al., 2012).

EXPERIMENTAL PROCEDURES

Generation of TRAP-1 Knockout Mice

All procedures involving animals were approved by an Institutional Animal Care and Use Committee (IACUC) at The Wistar Institute. A murine 129P2 ES clone E150H04, containing an insertional mutation downstream of the first exon of the TRAP-1 gene (rFlipROSAßgeo vector) was obtained from the German Gene Trap Consortium. Splinkerette PCR sequence of the ES clone is available at http://www.ncbi.nlm.nih.gov/nucgss/FI570935.1. Following pronuclear injections, zygotes were transferred to pseudopregnant C57BL/6 female mice and resulting chimeric male mice were crossed with C57BL/6 females to obtain mice heterozygous for the insertional mutation. The colony was maintained on a mixed B6/129 background by brother × sister mating.

Statistical Analysis

Data were analyzed using the two-sided unpaired t tests using a GraphPad software package (Prism 4.0) for Windows. The Kolmogorov-Smirnov two-sample test was used to analyze standardized uptake values (SUVs) in WT and TRAP-1$^{-/-}$ mice in PET/CT experiments using StatXact 9. Data are expressed as mean ± SD or mean ± SEM of replicates from a representative experiment out of at least three independent determinations. A p value of <0.05 was considered as statistically significant.

SUPPLEMENTAL INFORMATION

Supplemental Information includes Supplemental Experimental Procedures and four figures and can be found with this article online at http://dx.doi.org/10.1016/j.celrep.2014.06.061.

ACKNOWLEDGMENTS

This work was supported by NIH grants P01 CA140043 (D.C.A., L.R.L.), R01 CA78810 (D.C.A.), R01 CA089720 (L.R.L.), and the Office of the Assistant Secretary of Defense for Health Affairs through the Prostate Cancer Research Program under Award No. W81XWH-13-1-0193 (D.C.A.). Support for Core Facilities utilized in this study was provided by Cancer Center Support Grant (CCSG) CA010815 to The Wistar Institute.

Received: April 7, 2014
Revised: June 6, 2014
Accepted: June 28, 2014
Published: July 31, 2014

REFERENCES

Agorreta, J., Hu, J., Liu, D., Delia, D., Turley, H., Ferguson, D.J., Iborra, F., Pajares, M.J., Larrayoz, M., Zudaire, I., et al. (2014). TRAP1 regulates proliferation, mitochondrial function, and has prognostic significance in NSCLC. Mol. Cancer Res. *12*, 660–669.

Altieri, D.C., Stein, G.S., Lian, J.B., and Languino, L.R. (2012). TRAP-1, the mitochondrial Hsp90. Biochim. Biophys. Acta *1823*, 767–773.

Balch, W.E., Morimoto, R.I., Dillin, A., and Kelly, J.W. (2008). Adapting proteostasis for disease intervention. Science *319*, 916–919.

Butler, E.K., Voigt, A., Lutz, A.K., Toegel, J.P., Gerhardt, E., Karsten, P., Falkenburger, B., Reinartz, A., Winklhofer, K.F., and Schulz, J.B. (2012). The mitochondrial chaperone protein TRAP1 mitigates α-Synuclein toxicity. PLoS Genet. *8*, e1002488.

Butow, R.A., and Avadhani, N.G. (2004). Mitochondrial signaling: the retrograde response. Mol. Cell *14*, 1–15.

Caino, M.C., Chae, Y.C., Vaira, V., Ferrero, S., Nosotti, M., Martin, N.M., Weeraratna, A., O'Connell, M., Jernigan, D., Fatatis, A., et al. (2013). Metabolic stress regulates cytoskeletal dynamics and metastasis of cancer cells. J. Clin. Invest. *123*, 2907–2920.

Chae, Y.C., Caino, M.C., Lisanti, S., Ghosh, J.C., Dohi, T., Danial, N.N., Villanueva, J., Ferrero, S., Vaira, V., Santambrogio, L., et al. (2012). Control of tumor bioenergetics and survival stress signaling by mitochondrial HSP90s. Cancer Cell *22*, 331–344.

Chae, Y.C., Angelin, A., Lisanti, S., Kossenkov, A.V., Speicher, K.D., Wang, H., Powers, J.F., Tischler, A.S., Pacak, K., Fliedner, S., et al. (2013). Landscape of the mitochondrial Hsp90 metabolome in tumours. Nat. Commun. *4*, 2139.

Costa, A.C., Loh, S.H., and Martins, L.M. (2013). Drosophila Trap1 protects against mitochondrial dysfunction in a PINK1/parkin model of Parkinson's disease. Cell Death Dis. *4*, e467.

Ellis, R.J. (2007). Protein misassembly: macromolecular crowding and molecular chaperones. Adv. Exp. Med. Biol. *594*, 1–13.

Frezza, C., Zheng, L., Folger, O., Rajagopalan, K.N., MacKenzie, E.D., Jerby, L., Micaroni, M., Chaneton, B., Adam, J., Hedley, A., et al. (2011). Haem oxygenase is synthetically lethal with the tumour suppressor fumarate hydratase. Nature *477*, 225–228.

Gorgoulis, V.G., Vassiliou, L.V., Karakaidos, P., Zacharatos, P., Kotsinas, A., Liloglou, T., Venere, M., Ditullio, R.A., Jr., Kastrinakis, N.G., Levy, B., et al. (2005). Activation of the DNA damage checkpoint and genomic instability in human precancerous lesions. Nature *434*, 907–913.

Guarente, L. (2008). Mitochondria—a nexus for aging, calorie restriction, and sirtuins? Cell *132*, 171–176.

Guertin, D.A., and Sabatini, D.M. (2007). Defining the role of mTOR in cancer. Cancer Cell *12*, 9–22.

Haq, R., Shoag, J., Andreu-Perez, P., Yokoyama, S., Edelman, H., Rowe, G.C., Frederick, D.T., Hurley, A.D., Nellore, A., Kung, A.L., et al. (2013). Oncogenic BRAF regulates oxidative metabolism via PGC1α and MITF. Cancer Cell *23*, 302–315.

Janiszewska, M., Suvà, M.L., Riggi, N., Houtkooper, R.H., Auwerx, J., Clément-Schatlo, V., Radovanovic, I., Rheinbay, E., Provero, P., and Stamenkovic, I. (2012). Imp2 controls oxidative phosphorylation and is crucial for preserving glioblastoma cancer stem cells. Genes Dev. *26*, 1926–1944.

Kang, B.H., Plescia, J., Dohi, T., Rosa, J., Doxsey, S.J., and Altieri, D.C. (2007). Regulation of tumor cell mitochondrial homeostasis by an organelle-specific Hsp90 chaperone network. Cell *131*, 257–270.

Kimmelman, A.C. (2011). The dynamic nature of autophagy in cancer. Genes Dev. *25*, 1999–2010.

Lavery, L.A., Partridge, J.R., Ramelot, T.A., Elnatan, D., Kennedy, M.A., and Agard, D.A. (2014). Structural asymmetry in the closed state of mitochondrial Hsp90 (TRAP1) supports a two-step ATP hydrolysis mechanism. Mol. Cell *53*, 330–343.

Liang, J., and Mills, G.B. (2013). AMPK: a contextual oncogene or tumor suppressor? Cancer Res. *73*, 2929–2935.

Lu, C., Ward, P.S., Kapoor, G.S., Rohle, D., Turcan, S., Abdel-Wahab, O., Edwards, C.R., Khanin, R., Figueroa, M.E., Melnick, A., et al. (2012). IDH mutation impairs histone demethylation and results in a block to cell differentiation. Nature *483*, 474–478.

Merksamer, P.I., Liu, Y., He, W., Hirschey, M.D., Chen, D., and Verdin, E. (2013). The sirtuins, oxidative stress and aging: an emerging link. Aging (Albany, N.Y. Online) *5*, 144–150.

Nisoli, E., Tonello, C., Cardile, A., Cozzi, V., Bracale, R., Tedesco, L., Falcone, S., Valerio, A., Cantoni, O., Clementi, E., et al. (2005). Calorie restriction promotes mitochondrial biogenesis by inducing the expression of eNOS. Science *310*, 314–317.

Pridgeon, J.W., Olzmann, J.A., Chin, L.S., and Li, L. (2007). PINK1 protects against oxidative stress by phosphorylating mitochondrial chaperone TRAP1. PLoS Biol. *5*, e172.

Schulz, T.J., Zarse, K., Voigt, A., Urban, N., Birringer, M., and Ristow, M. (2007). Glucose restriction extends Caenorhabditis elegans life span by inducing mitochondrial respiration and increasing oxidative stress. Cell Metab. *6*, 280–293.

Sciacovelli, M., Guzzo, G., Morello, V., Frezza, C., Zheng, L., Nannini, N., Calabrese, F., Laudiero, G., Esposito, F., Landriscina, M., et al. (2013). The mitochondrial chaperone TRAP1 promotes neoplastic growth by inhibiting succinate dehydrogenase. Cell Metab. *17*, 988–999.

Selak, M.A., Armour, S.M., MacKenzie, E.D., Boulahbel, H., Watson, D.G., Mansfield, K.D., Pan, Y., Simon, M.C., Thompson, C.B., and Gottlieb, E. (2005). Succinate links TCA cycle dysfunction to oncogenesis by inhibiting HIF-alpha prolyl hydroxylase. Cancer Cell *7*, 77–85.

Taipale, M., Jarosz, D.F., and Lindquist, S. (2010). HSP90 at the hub of protein homeostasis: emerging mechanistic insights. Nat. Rev. Mol. Cell Biol. *11*, 515–528.

Turcan, S., Rohle, D., Goenka, A., Walsh, L.A., Fang, F., Yilmaz, E., Campos, C., Fabius, A.W., Lu, C., Ward, P.S., et al. (2012). IDH1 mutation is sufficient to establish the glioma hypermethylator phenotype. Nature *483*, 479–483.

Wallace, D.C. (2012). Mitochondria and cancer. Nat. Rev. Cancer *12*, 685–698.

Ward, P.S., and Thompson, C.B. (2012). Metabolic reprogramming: a cancer hallmark even warburg did not anticipate. Cancer Cell *21*, 297–308.

Yoshida, S., Tsutsumi, S., Muhlebach, G., Sourbier, C., Lee, M.J., Lee, S., Vartholomaiou, E., Tatokoro, M., Beebe, K., Miyajima, N., et al. (2013). Molecular chaperone TRAP1 regulates a metabolic switch between mitochondrial respiration and aerobic glycolysis. Proc. Natl. Acad. Sci. USA *110*, E1604–E1612.